MICROCOPY RESOLUTION TEST CHART

MTL TR 87-3

AD

SYNTHESIS AND PROPERTIES OF ALIPHATIC POLYURETHANES AND MODEL COMPOUNDS CONTAINING $\alpha,\alpha,\alpha',\alpha'$-TETRAMETHYL-p-XYLYLENE-DIISOCYANATE

BRIAN A. ZENTNER
MATERIALS CHARACTERIZATION DIVISION

January 1987

Approved for public release; distribution unlimited.

DTIC
ELECTE
MAR 2 6 1987
S E D

US ARMY
LABORATORY COMMAND
MATERIALS TECHNOLOGY
LABORATORY

U.S. ARMY MATERIALS TECHNOLOGY LABORATORY
Watertown, Massachusetts 02172-0001

87 3 25 046

REPORT DOCUMENTATION PAGE		READ INSTRUCTIONS BEFORE COMPLETING FORM
1. REPORT NUMBER MTL TR 86-3	2. GOVT ACCESSION NO. AD-AM831?	3. RECIPIENT'S CATALOG NUMBER
4. TITLE *(and Subtitle)* SYNTHESIS AND PROPERTIES OF ALIPHATIC POLYURETHANES AND MODEL COMPOUNDS CONTAINING α,α,α',α'-TETRAMETHYL-p-XYLYLENE-DIISOCYANATE		5. TYPE OF REPORT & PERIOD COVERED Final Report
		6. PERFORMING ORG. REPORT NUMBER
7. AUTHOR(s) Brian A. Zentner		8. CONTRACT OR GRANT NUMBER(s)
9. PERFORMING ORGANIZATION NAME AND ADDRESS U.S. Army Materials Technology Laboratory Watertown, Massachuetts 02172-0001 ATTN: SLCMT-OMM		10. PROGRAM ELEMENT, PROJECT, TASK AREA & WORK UNIT NUMBERS D/A Project: 1L162105AH84 Agency Acc. Number: DA304096
11. CONTROLLING OFFICE NAME AND ADDRESS U.S. Army Laboratory Command 2800 Powder Mill Road Adelphi, Maryland 20783-1145		12. REPORT DATE January 1987
		13. NUMBER OF PAGES 98
14. MONITORING AGENCY NAME & ADDRESS(if different from Controlling Office)		15. SECURITY CLASS. (of this report) Unclassified
		15a. DECLASSIFICATION/DOWNGRADING SCHEDULE

16. DISTRIBUTION STATEMENT *(of this Report)*

Approved for public release; distribution unlimited.

17. DISTRIBUTION STATEMENT *(of the abstract entered in Block 20, if different from Report)*

18. SUPPLEMENTARY NOTES

(SEE REVERSE SIDE)

19. KEY WORDS *(Continue on reverse side if necessary and identify by block number)*

Polyurethanes,
X-ray crystallography,
Fatigue (mechanics),
Thermal analysis

Synthetic rubber's
Synthesis (chemistry)

20. ABSTRACT *(Continue on reverse side if necessary and identify by block number)*

(SEE REVERSE SIDE)

DD `FORM 1 JAN 73` 1473 EDITION OF 1 NOV 65 IS OBSOLETE

Block No. 18

Preliminary report presented at the 129th meeting of the Rubber Division, American Chemical Society, New York, NY, April 8-11, 1986.

Reprinted as submitted to the Boston University Graduate School, in partial fulfillment of the requirements for the degree of Doctor of Philosophy, 1987.

Block No. 20

ABSTRACT

New materials are needed to replace the rubber compounds which are in current use in certain high stress environments. The rubber materials usually fail due to the high internal temperature which results from compressive cycling under heavy loads. Rubber formulations, such as styrene-butadiene, also fail due to severe mechanical stresses, such as tearing forces.

Polyurethanes are being examined as possible replacements due to indications of better mechanical strength. However, hysteric heat buildup in polyurethanes is a major problem. The compound $\alpha,\alpha,\alpha',\alpha'$-tetramethyl-p-xylylene-diisocyanate (p-TMXDI) was examined as a viable component in polyurethanes. Poly-(1,4-butanediol) of two high molecular weights was used as the soft segment, with 1,4 butanediol, resorcinol-1,3-bis(β-hydroxyethyl)ether, and 4,4'-isopropylidenediphenol-4,4'-bis(β-hydroxyethyl)ether tested individually as chain extenders and 2-ethyl-2-(hydroxymethyl)-1,3-propandiol and triethanolamine used as crosslinkers. Mechanical and thermal measurements were made on polymers prepared with various ingredient types and ratios. Investigation of the molecular arrangement of the polyurethane samples was made using infrared and X-ray scattering techniques. Low molecular weight model compounds, simulating the polar regions of the polyurethanes, were prepared and characterized by single crystal X-ray diffraction by Dr. Jerry P. Jasinski. Compressive fatigue tests were conducted on some samples which showed good thermal resistance by other tests.

The properties of p-TMXDI-based polyurethanes are comparable to other polyurethane classes. When 1,4-butanedoil was the chain extender, the samples possessed good tensile and tear strength and low glass transition temperatures, with high-temperature softening above 150°C. Compressive fatigue tests on block samples demonstrated the resistance of these polyurethanes to the buildup of high internal temperatures which would cause failure of the polymer.

The model compounds of p-TMXDI provided information on the possible conformation of this unique structure in the polyurethane chains. Until recently, polyurethanes made from diphenylmethane-4,4'-diisocyanate were the only polyurethane class which had been characterized by X-ray scattering and X-ray crystallographic techniques. *(Keywords:)*

LIST OF FIGURES

LIST OF FIGURES (cont.)

LIST OF TABLES

Accession For

NTIS

A-1

DTIC
COPY
INSPECTED

CONTENTS

I. INTRODUCTION

This research project has been motivated by the need for an elastomer which can resist severe cyclic stresses for prolonged periods. Among elastomers used in applications such as solid tires are styrene-butadiene rubber (SBR) block copolymers. SBR has proved useful for environments of moderate stress, but has proved to be inadequate for heavy loads which cause increased abrasion on the road surface, chunking (loss of elastomer pieces), fatigue from internal heat buildup, or a combination of these stresses. Catastrophic failure (e.g. internal melting or "explosion" of the elastomer) is sometimes the result of these severe stresses.

Polyurethane elastomers offer some desirable properties as a substitute material. Some provide higher strength than SBR and demonstrate excellent abrasion resistance. A major disadvantage noted in the testing of most polyurethane samples is the higher hysteresis (internal heatup) of test blocks compared to SBR blends. Efforts have been conducted to find polyurethane blends with hysteresis low enough to survive the severe stress of cyclic testing.

Recent test results have indicated that polyurethane block copolymers having low hysteretic heatup behavior can be produced. Samples containing an aliphatic diisocyanate (cyclohexyl diisocyanate) (CHDI) have developed the lowest hysteretic heatup of any class of polyurethane tests which were reported prior to the work described in this thesis. This property of thermal stability is believed to be due to the high

1

symmetry of the segments containing urethane bonds derived from CHDI. The symmetry allows formation of highly crystalline (and thus "high" temperature melting) regions in the CHDI-based polyurethanes.

p-TMXDI (para-tetramethylxylene diisocyanate) is an aliphatic diisocyanate, with propylidine groups separating the isocyanate groups from the central aromatic ring, which, based on its comparison with the structure of CHDI, should also produce regions of some symmetry. Although the urethane bonds in the p-TMXDI-based polyurethanes are somewhat hindered, crystalline (and possibly "high" temperature melting) regions are postulated for these materials. This is the premise on which this research is based.

The research involves the preparation of polyurethane samples with incremental changes in content of p-TMXDI, soft-segment molecular weight, and hard-segment chain extender and crosslinker types and percentages. The thermal, mechanical, and structural characteristics of the samples were examined by several methods to determine the sample preparations which displayed preferred behavior (e.g. softening temperature $>150^{o}$C) and possible structure-property relationships.

II. LITERATURE SURVEY

A. Phase Separation

Polyurethanes are formulated for many different purposes such as coatings, insulation, and shock absorbing components. The focus of this research is upon elastomeric behavior, wherein a polymer is neither rigid and brittle (glasslike) nor permanently deformed by stretching (such as plastic food wrap), but has a tendency to return to its original shape after removal of the force causing deformation. Within the polymer class of elastomers is a subclass termed block copolymers. Styrene-butadiene polymers are an example, where a length of styrene units (about 50-100) is connected to a length of butadiene units (about 50-100). The polymer is cured so that the hard styrene lengths associate to form inflexible regions which hold together the various flexible butadiene chains. In this way the styrene regions reinforce the elastomeric butadiene chains and prevent permanent deformation of the polymer. Cooper and Tobolsky[1] first pointed out similarities between polyurethanes and styrene-isoprene block copolymers in the way they form specific domain structures.

Polyurethane chains are composed of polar and non-polar repeating sections, with the length of each repeat dependent upon the number of molar equivalents of diisocyanate incorporated into the polar section and the average molecular weight of long chain diol chosen for the non-polar section. During the curing process a two phase system develops, mainly due to the differences in polarity of each section of each

chain. The extent to which these phases separate is influenced by various factors. Some common diisocyanates are shown in Fig. 1. Schneider and Sung[2] found an increase in soft segment T_g (glass transition temperature) for samples containing higher percentages of 2,4-TDI (toluene diisocyanate) in a polyester soft segment matrix; T_g was also increased in lower molecular weight polyethers, the shorter chains allowing less free movement of the polar regions during the cure process. In the 2,6-TDI samples, however, it was found that only the lower molecular weight polyesters (i.e. mw<2000) developed a T_g increase as hard segment percentage was increased, and to a more limited extent than 2,4-TDI. One factor assumed to be influencing these differences was the higher symmetry of the 2,6-TDI unit compared to the 2,4-TDI unit, leading to a greater probability of crystalline hard segments in a 2,6-TDI-based polyurethane, which would represent a better driving force for phase separation. Chen et al.[3-4] noted that the HTPBD (hydroxy-terminated polybutadiene) T_g was essentially unaffected by variations in the percentage of hard segment material. Camberlin and Pascault[5-6] found a lower tendency for phase mixing for hydrogenated HTPBD than for the unsaturated analogues. These and other results[7] indicated that a decreasing polarity in the soft segment chains leads to less phase mixing, i.e. the tendency of hard and soft regions to mix is: polyester > polyether > polybutadiene > hydrogenated polybutadiene. (Phase mixing causes an increase in T_g of the soft segment compared to the T_g of the pure soft segment material because of the much higher T_g

4

Figure 1. Diisocyanates

OCN⟨○⟩CH$_2$⟨○⟩NCO   MDI
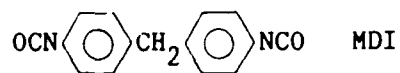
methylene-bis(phenylisocyanate)
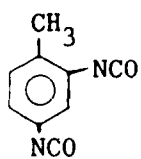
2,4-TDI   2,6-TDI

toluene diisocyanate

OCN⟨ ⟩CH$_2$⟨ ⟩NCO   H$_{12}$MDI
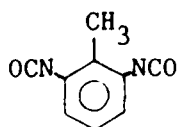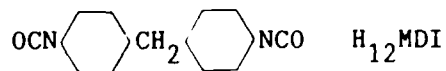
methylene-bis(cyclohexylisocyanate)

CHDI   (>99% trans)

cyclohexyldiisocyanate

5
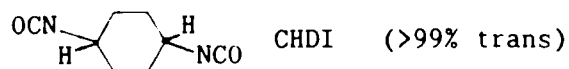
of hard segment material.) The method of preparation also has some influence on phase separation. Miller et al.[8] prepared MDI/BD/PTMO samples by one step (all ingredients at once) and two step (MDI/PTMO prepolymer, then BD (butanediol) chain extender) methods. The two step samples were found to contain more individual isolated MDI hard segments. The single units were more likely to phase mix with the PTMO chains, thus leading to less phase separation in the two step polymers. However, in the case of a polyester soft segment, Abouzahr and Wilkes[9] reported poorer properties for a one step synthesis due to the higher compatibility of the hard segments with the polyester carbonyls and thus poorer phase separation. Samples with higher molecular weight polyether soft segment, prepared in a one step synthesis and tested by van Bogart et al.[10], had better phase separation than lower MW samples. Longer soft segment chains have also promoted better phase separation in other polyurethane systems[1]. Miller and Cooper[11] noted SAXS (small angle X-ray scattering) and DSC (differential scanning calorimetry) evidence which indicated improved phase separation as curing temperature was increased, allowing greater mobility of the polymer chains, which permitted better association of chain segments. (Importance of phase separation is dependent upon desired properties: e.g., phase separation in foam insulation may have little effect upon performance, while shock absorbers may depend upon well separated phases for long life.)

In summary, the following factors may influence phase separation: polarity of the soft segment material, molecular weight (relative length) of the soft segment, number of equivalents of the hard segment (i.e. hard segment %/soft segment % ratio by weight), method of prepa-

6

ration (one step or two step), curing temperature, symmetry and crystallinity of the hard segment, and hydrogen bonding. Among the methods used to characterize the phase separation are X-ray studies, thermal analysis, infrared spectroscopy, and mechanical testing. With the availability of various soft segments, diisocyanates, chain extenders, and crosslinking agents, thousands of combinations are possible. This illustrates the need for the above test methods and other methods to fully characterize each polyurethane preparation.

B. Infrared Spectroscopy

Infrared techniques have made significant contributions to the examination of phase separation and other properties in polyurethanes. In a detailed review, West and Cooper[12] discussed the observations[13-14] that most polyurethanes had signs of almost complete hydrogen bonding of N-H functions but varying involvements (about 65%-90%) of urethane carbonyls toward hydrogen bonding in different preparations. Evidence indicated some participation in the hydrogen bonding by polyether oxygens[14], carbonyls (in polyesters), and possibly C-O-C (alkoxy) oxygens in other urethane moieties[13]. The influences of hard segment-soft segment hydrogen bonds therefore are a major factor in the phase separation which develops during the polyurethane cure. However, hydrogen bonding is not an essential property for a polyurethane. Harrell[15] prepared polyurethanes having hard segments incapable of hydrogen bond-

7

ing; these samples showed the same types of behavior as conventional polyurethane block copolymers due to the crystallization of the hard segment regions.

Observation of changes in hydrogen bonding permits the monitoring of structural changes during the application of various stresses to polyurethane samples. Some evidence indicates breakage of a small percentage of hydrogen bonds during elongation and their subsequent return with time after relaxation[14]. Increasing the temperature of various samples caused the breaking of most hard-soft-segment hydrogen bonds before the interurethane hydrogen bonds, indicating that the hard-soft hydrogen bonds are somewhat weaker than hard-hard segment hydrogen bonds and giving some measure of the phase mixing and hard-soft segment interaction.[16] Similar studies on deformation and temperature effects have been performed by Burchell et al.[17a-f]. Siesler[18], who has tested polyurethanes by thermal and mechanical means correlated with FTIR measurements, has also flushed samples with gaseous D_2O for hydrogen exchange; this has permitted some estimation of hard segment percentage mixed in soft segment regions since crystalline hard segment N-H's are less susceptible to deuterium exchange.

Recent work by Coleman et al.[19-21] demonstrates that the previous interpretations of temperature dependence of hydrogen bonds, using N-H absorptions, has been erroneous. The absorption intensity of "free" N-H has previously been a guide to the percentage of hydrogen bonding present as the temperature increases. It has been observed that "the mean strength of the hydrogen bonds decreases with increasing temperature."[21]

Also, "the absorptivity coefficient is a strong function of the strength of the hydrogen bond and varies significantly as the band shifts in frequency"[21], giving the false indication that "additional" hydrogen bonds are being broken as temperature rises. The percentage of "free" N-H groups actually does not increase significantly until at least 200°C. Also, the temperature increase causes a spread of the distribution of absorption energies in the N-H stretching region, thus complicating any quantitative interpretations of changes in hydrogen bonding by IR measurement of the N-H region due to these frequency shifts. These factors result in a smaller area for the hydrogen bonded N-H band.

C. Thermal Behavior

The behavior of polyurethanes at different temperatures has a direct bearing upon their applications; at operating temperatures, elastomers must have a soft segment which is not brittle (glassy) and a hard segment structure which will not soften or melt from thermal, mechanical, or a combination of stresses. Various thermal transitions in polyurethanes have been identified by researchers. For example, Hesketh, van Bogart, and Cooper[22], in examining various types of polyurethanes, characterized several distinct transitions by DSC:

1. T_g, the soft segment glass transition. In this region a polymer soft segment changes from a hard brittle material to a soft flexible material as the temperature rises. Its value is usually a measure of

9

phase mixing, as the T_g is increased by the presence of impurities such as hard segment chains. Different soft segments have different T_g's depending upon type and molecular weight.

2. T_{ms}, the soft segment melting transition. This is occasionally present if conditions are suitable for some alignment and crystallization of the long soft segment chains. Its probability would be enhanced by the absence of interfering hard segments, i.e. more phase separation.

3. T_{gh}, the hard segment glass transition. This is detectable only in some polyurethanes.

4. Amorphous melting transitions caused by hard segment domains of short and long range order (i.e., amorphous hard segment regions with small isolated sections with less than crystalline order). The existence and extent of amorphous hard segment regions depends upon their tendency to crystallize, the molecular weight of the soft segment, the percentage of hard segment material, and other factors.

5. T_m, the hard segment melting transition. This is present if hard segments crystallize. This may indicate the temperature at which the polyurethane will soften and fail, or it may merely indicate the presence of some crystalline regions. The final softening temperature is dependent upon the mixture of amorphous and crystalline hard segment regions present in any particular polyurethane, and thus could be lower than T_m.

Harrell[15], in his experiments with monodisperse hard segment sizes, noted that an increase in the number of units in a hard segment chain caused a corresponding increase in the T_m. Also, mixing polyurethanes

10

with different lengths of hard segment chains produced a material in which the separate T_m's were still present for each characteristic length. This indicated that, provided the hard segments had a narrow length distribution, separate distinctive T_m's were possible for a crystalline material.

Ordering (phase separation and crystallinity) of the segments after completion of the polymerization may also be influenced by annealing at temperatures above the reaction temperature. Annealing at various temperatures, for various times, up to just below the T_m for a polyurethane caused the T_m to increase (after annealing) by about 10^oC-20^oC[22-26]. This was an indication of increased ordering of the hard segment regions. Annealing above T_m usually caused a short term disruption which was reversed with time after cooling and sometimes produced better ordering[22-24].

D. Mechanical Testing

The mechanical behavior of a polyurethane is a reflection of its chemical content and phase separation. Zdrahala et al.[27] observed an increase in the hardness, tensile strength, and tear strength of samples in a polyurethane class with a variation in the percentage of hard segment material from 20% to 80%. Above 60% hard segment content, however, the tensile and elongation properties decreased, indications of a transition from a tough elastomer to a brittle plastic. Chang et al.[28] noted similar results for tensile and elongation properties and observed, by optical and electron microscopy, the various polyurethane

11

structural regions which develop as the hard segment content is varied. Harrell[15] prepared samples with broad hard segment size distributions and found poorer stress/strain and elongation properties than for samples in which the hard segment length was kept in a narrow range. Other behavior, such as abrasion resistance and dynamic mechanical (resistance to flexing at various temperatures), is dependent upon phase mixing and chain packing for both hard and soft segments.

E. X-ray Scattering Analysis

Determination of hard segment chain conformation and relative size of hard segment regions has been a primary endeavor of researchers interested in establishing a structure-property relationship in some polyurethanes. Electron microscopy experiments provided estimations of hard segment size and extent[28], but there is some disagreement about the interpretations of the various regions. Also, the process of electron microscopy, i.e. the use of the electron beam, causes modification of the material during the scanning. Methods for enhancing surface contrast (sputtering, heavy metal staining) are dependent upon differences in polarity, surface texture, or the presence of aliphatic double bonds in the hard and soft regions, properties which are sometimes not sufficiently different to produce good contrast. X-ray scattering is a direct measure of electron density which allows calculation of average size of the hard segment regions and measurement of crystallinity.

Small angle X-ray scattering data provides some estimation of domain size, distance between domains, and the size of domain transition

regions, i.e. the regions where some phase mixing occurs due to the uneven alignment of packed chains or the incomplete phase separation which occurs in most polyurethanes. Wilkes and Yusek[29] measured a domain separation (center to center) for MDI/BD, with a polyester (mol.wt.$\simeq$ 1000) soft segment, of 150 Å; another sample polyester (of mol.wt.$\simeq$ 2000) yielded an average separation of 220 Å. Schneider et al.[30] analysed several MDI/BD samples with a polyether (mol.wt.$\simeq$ 2000) soft segment and noted a spacing of from 182 to 210 Å in the various preparations. Fulcher and Corbett[31] prepared MDI/BD samples with polyether (mol.wt.$\simeq$ 1000) and found domain sizes (diameter) of 50-100 Å with separations (center to center) of 100-170 Å. Ophir and Wilkes[32] measured some polyester interfacial thicknesses (phase transition zones) of 10-12 Å and polyether of 5-7 Å, indicating better phase separation for the polyethers.

Wide angle X-ray scattering is suitable for determining relative percentage of crystallinity and identifying some crystalline reflections useful for predicting chain conformation. Bonart et al.[33] first proposed a conformational arrangement for MDI/BD based upon WAXS (wide angle X-ray scattering) reflections from polyurethanes with polyester soft segments; the model accounted for the hydrogen bonding arrangement and the possible long range ordering of adjacent chains. Later Bonart et al.[34] developed models for butanediol- and pentanediol-extended MDI polyurethanes which depended upon a three-dimensional hydrogen bonding network for hard segment "virtual crosslinking." These models were based on the assumption that the hard segments, when crystalline, were composed of relatively straight chains. Koberstein et al.[35-37] determined,

13

mostly from SAXS, that longer hard segment chains (e.g. 3 or more MDI units) assumed some folded configurations, i.e. the butanediol section provided sufficient flexibility for the chain to curve back into the hard segment region at the phase boundary. This model was proposed to account for some increased boundary thicknesses and some amorphous DSC melting transitions (due to amorphous hard segment regions).

F. Model Compounds Characterization

X-ray scattering experiments on oriented films of polyurethanes has enabled researchers to propose some model conformations for the hard segment regions. The bulk of this work has involved mostly MDI, mainly because of its commercial dominance, and partly due to the varied evidence of hard segment crystallinity. However, the variation in spacings calculated from reflections on different samples has generated different proposals concerning the exact conformation of the hard segment chains. Evidence exists for two, and perhaps more, possible conformations of MDI and butanediol hard segments. To assist the resolution of these complicated structures, low molecular weight model compounds have been prepared which simulate different sections of the hard segment chain with different chain extenders. When possible, single crystals have been grown, and X-ray diffraction measurements on these crystals have prov'ded information on bond lengths, bond angles, torsion angles, and overall conformation suitable for extrapolation into longer chains.

The first published model was prepared and analyzed by Blackwell and Gardner[38] by reaction of MDI with methanol (Fig. 2). The crystal was

14

nearly orthorhombic ($\gamma=93.9^{\circ}$); after simulated addition of two $-CH_2-$ functions to join adjacent methyl ends, the unit cell was distorted into a triclinic shape ($\alpha=115^{\circ}$, $\beta=121^{\circ}$, $\gamma=85^{\circ}$). This agreed closely with the pattern from an oriented film ($\alpha=116^{\circ}$, $\beta=116^{\circ}$, $\gamma=83.5^{\circ}$)[39]. Further conformational analyses were performed on models extended by ethylene glycol[40-43], propanediol[40-43], butanediol[40-44], and hexanediol[41-43,45].

Other crystal model compounds followed this initial study. Hocker and Born[46] grew a second crystal conformation from Blackwell's model compound; this crystal fit a different space group than the first crystal and represented a chain stacking which is not seen in stretched films of polyurethane. Born et al.[47] later prepared a monofunctional analogue of MDI (MMI, a monoisocyanate), two molecules of which were joined by chain extenders $HO-(CH_2)_x-OH$, where $x=2$ to 6 (Fig. 2). A crystal structure of the butanediol extended model was obtained[48] which was in close agreement with the analysis of Blackwell's model. Bonart's model[33] is comparable to the results derived from the model compounds with regard to general packing orientation, but the predicted chain staggering in the longitudinal direction implied separation between the chains which was "unrealistically small"[47]. Work on the model compounds by both groups[49] supplied data for average bond lengths, bond angles, and torsion angles.

Model compounds are also guides to thermal behavior properties. DSC experiments on model compounds with increasing numbers of MDI units show increasing melting temperatures; this is especially true when the ends are long chains such as octadecanol (end caps)[50]. DSC scans also show the highest melting temperatures occur when the chain extender is

butanediol[51].

Recent work by Briber and Thomas[52-53] has revealed two different crystal conformations in MDI-based polyurethanes. Along with highly disordered regions, which they labeled Type I, a crystalline form (Type II) was found with a "contracted" repeat distance of 17 Å. In oriented stretched films of the same blends, the "fully extended" (Type III) repeat distance was found to be 19 Å. This, along with other evidence, indicates that mechanical history, along with other factors mentioned previously, has an effect on the morphology and resulting behavior of a polyurethane.

Figure 2. Model Compounds of MDI
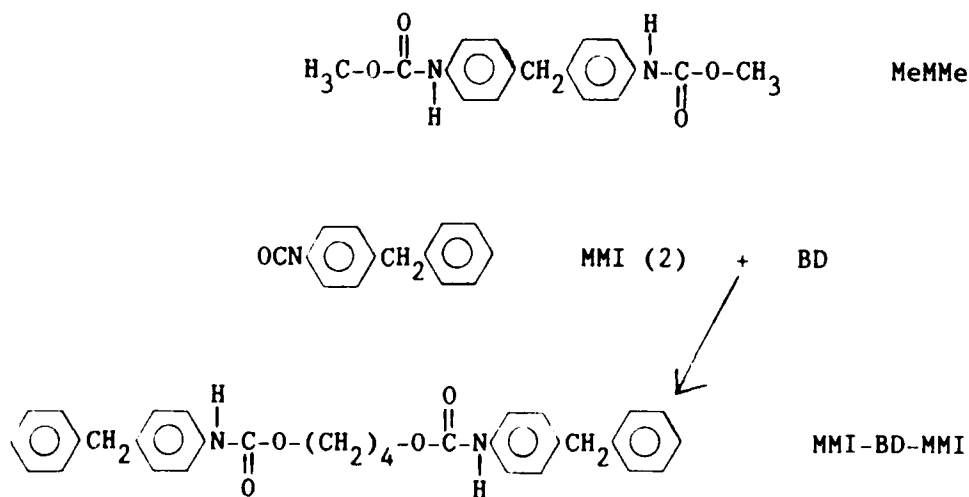
III. MONOMER SURVEY

A. Soft Segment Material

Selection of a polyurethane soft segment material is usually based upon the desired mechanical and thermal properties of the resulting polymer. Materials used as soft segments can be classed as polyethers, polyesters, polybutadienes (including hydrogenated soft segments), polysiloxanes, and other less common types. Variations in molecular weight will also affect properties; higher molecular weight soft segments generally result in lower T_g's for polyurethanes. When comparing different types of polyethers and polyesters, PTMO of mol.wt.$\approx$2000 or greater retained its flexibility to a lower temperature than PTMO of mol.wt.<2000[54]. For this reason, and also to promote phase separation, PTMO was chosen as the soft segment for this research (Fig. 3).

B. Chain Extenders and Crosslinkers

To form the hard segment in a polyurethane, diisocyanates are linked to each other (in lengths of from 2 to 10 diisocyanate units) by short chain molecules; these hard segments are linked to the soft segments in hard-soft repeats which reach molecular weights of from 5,000 to 50,000. The short chain extenders are usually diols (for urethane bonds) or diamines (which will produce urea bonds). Some soft segments are available with terminal amine functional groups (in place of diols). This

17

Figure 3. Structures of Starting Materials

$$OCN-\underset{\underset{CH_3}{|}}{\overset{\overset{CH_3}{|}}{C}}-\langle\bigcirc\rangle-\underset{\underset{CH_3}{|}}{\overset{\overset{CH_3}{|}}{C}}-NCO \qquad \text{p-TMXDI}$$

$$HO-(CH_2)_4-OH \qquad \text{BD}$$

$$HO-(CH_2)_2-OH \qquad \text{EG}$$

$$HO-(CH_2)_6-OH \qquad \text{HD}$$

$$HO-CH_2-CH_2-O-\langle\bigcirc\rangle^{O-CH_2-CH_2-OH} \qquad \text{HER}$$

$$HO-CH_2-CH_2-O-\langle\bigcirc\rangle-\underset{\underset{CH_3}{|}}{\overset{\overset{CH_3}{|}}{C}}-\langle\bigcirc\rangle-O-CH_2-CH_2-OH \qquad \text{HEB}$$

$$HO-[-(CH_2)_4-O-]_x-H \qquad \text{PTMO}$$

$$H_3C-CH_2-C-(-CH_2-OH)_3 \qquad \text{TMP}$$

$$N(-CH_2-CH_2-OH)_3 \qquad \text{TEA}$$

$$HO-CH_2-CH_2-O-\langle\bigcirc\rangle-O-CH_2-CH_2-OH \qquad \text{HQEE}$$

$$(n-Bu)_2Sn(O_2C-(CH_2)_{10}-CH_3)_2 \qquad \text{DBTDL}$$
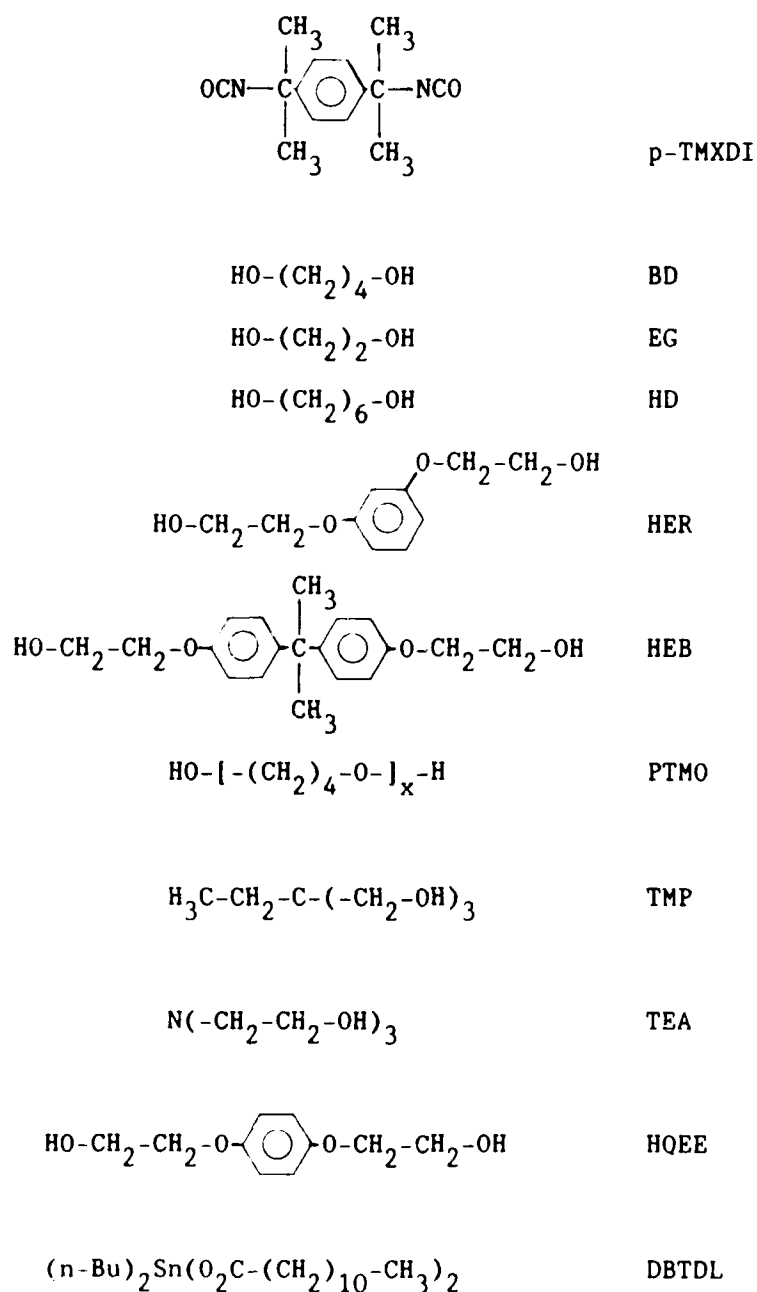
$x \approx 26.6$ for PTMO 1934; $x \approx 37.2$ for PTMO 2695

(abbreviations are defined in the Glossary on page 103)

18

expands the possible formulations from polyurethanes to polyureas and poly(urethaneureas). Due to the rapid reaction rate of amines, and to simplify the work, this study was confined to diol chain extenders and crosslinkers.

Besides the "virtual crosslinking" developed from hydrogen bonding, covalent crosslinking between different chains is available by various means. Allophanate crosslinks will develop under some conditions (e.g. low steric hindrance, excess diisocyanate). Biuret crosslinks are possible in polyureas. Some soft segment material is available as macrotriols, or it can be crosslinked by peroxides or other reagents. In the hard segment, low molecular weight triols or triamines can be added in specific amounts (to replace the appropriate amount of diol or diamine) to allow addition of known percentages of crosslinking.

A survey of aliphatic and aromatic diol chain extenders was conducted by Minoura et al.[55] They examined the mechanical properties of polyurethanes with these various chain extenders. From these results, three chain extenders were selected for use in this study: BD, HEB, and HQEE (Fig. 3). However, HQEE must be mixed at $120^{\circ}C$ or higher, a temperature too high to control the reaction rates in this study; therefore, HER was used as a substitute, since it also promotes retention of mechanical properties at elevated temperatures, as does HQEE[56].

For crosslinking of polyurethanes, TMP is the most widely used triol (Fig. 3). However, it is possible that TMP, which has some degree of steric hindrance, prevents a thorough polymerization of a diisocyanate which is hindered by α-methyl groups. For this reason, a switch was

19

made in this study to TEA, which is expected to be more reactive.

C. Diisocyanates

MDI (Fig. 1) is, at present, the most widely used diisocyanate for polyurethane manufacture. As noted already, its symmetry allows the ready development of crystalline hard segment regions with assorted overall properties dependent upon the blends of soft segments and chain extenders. However, when exposed to the environment, MDI is sensitive to ultraviolet light which yellows and degrades the performance of the polymer, as noted by Schollenberger and Stewart[57]; subsequently, Allen and McKellar[58] postulated the eventual degradation of the MDI unit to a di-quinone imide based upon ultraviolet evidence of a benzophenone-type impurity in photosensitive MDI-based polyurethanes (Fig. 4).

TDI is commonly available as a mixture of 80% 2,4-TDI and 20% 2,6-TDI; each of these isomers may also be obtained pure by separation. TDI, like MDI, exhibits a range of behaviors depending on the blends of the other polyurethane ingredients. Also, like MDI, it is sensitive to ultraviolet light and undergoes some photorearrangement[59] (Fig. 5).

H_{12}MDI is the saturated analogue of MDI. It is available as a mixture of 65% cis-trans, 30% trans-trans, and 5% cis-cis. Fractional crystallization allows removal of the trans-trans isomer and subsequent reblending for mixtures with from 10% to 95% of the trans-trans isomer. These isomer ratios lead to a wide variation in properties[60].

Figure 4. Photochemical Decomposition of MDI-based Polymers (Ref.58)
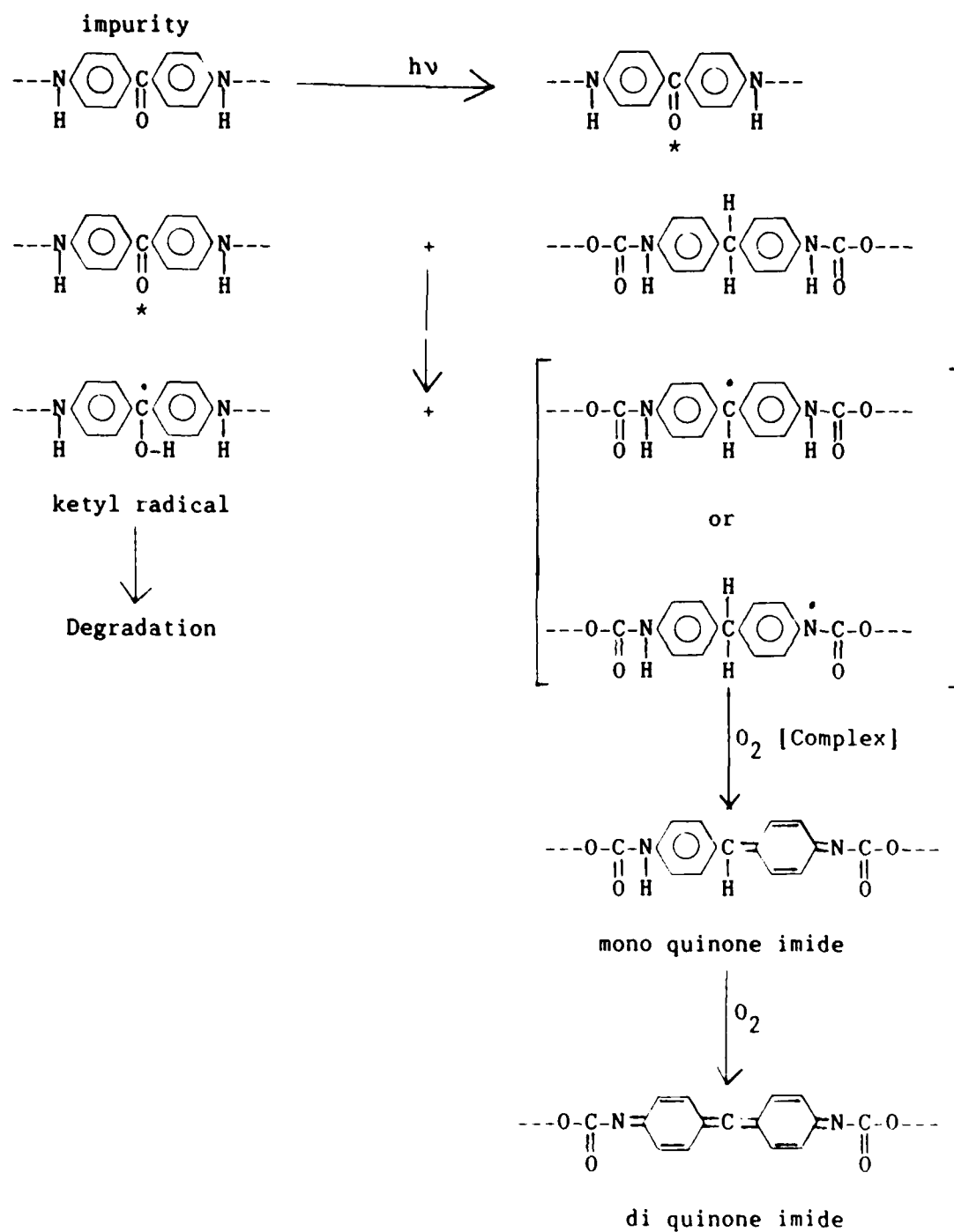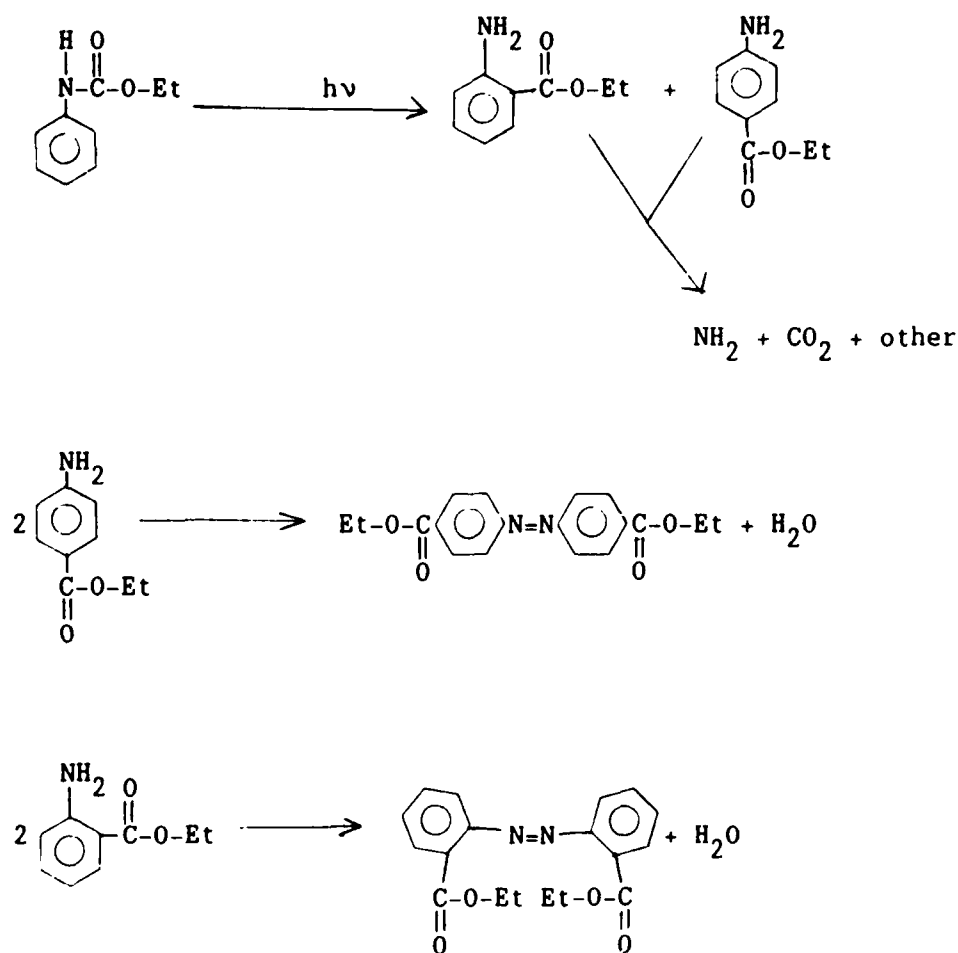
Figure 5. Photochemical Decomposition of TDI-type molecule (Ref.59)

(This is a photo-Fries rearrangement. Radical formation leading to quinoid-type products in 2,4- and 2,6-TDI-based polyurethanes is also possible.)

CHDI is a recently developed diisocyanate which has so far seen limited research. It is of primary interest due to CHDI-based polyurethanes which have shown excellent resistance to hysteretic heat buildup[61]. Some preliminary experiments suggest that preparation of model compounds will lead to an understanding of the properties of this polyurethane class.

TMXDI (Fig. 3) is a compound which is not yet in commercial production. It is available as either a meta or para isomer[62]. Only the para isomer was studied in this research. It is of interest because of the behavior of p-TMXDI based polyurethanes in thermal, mechanical, and hysteresis testing, and because of its unique structure and the ability of model compounds to crystallize in a unique conformation.

D. Catalysts

Polyurethanes are sometimes formed with the aid of catalysts, although the urethane forming reaction will take place slowly under some conditions (faster for aromatic NCO which need no catalyst). (Ureas will form rapidly without catalysts due to a different mechanism.) Among the available catalysts, tin-based formulas are among the best due to their high activity even at low concentrations (an increase of 30,000 to 50,000 in the reaction rate compared to uncatalyzed reactions). Many studies have been conducted on the mechanism of catalysis by tin-based formulas, resulting in some conflicting views on the sequence of events. The currently preferred mechanism involves an initial complex of two

23

catalyst molecules with two diol molecules[63]. DBTDL was used in this study due to its long chain carbalkoxy groups providing better solubility. Its formula is shown in Figure 3.

IV. EXPERIMENTAL METHODS

A. Synthesis

p-TMXDI was purified by vacuum distillation (135°C / 130 Pa, 1 Torr) and refrigerated under vacuum. DBTDL catalyst was diluted to 4% in methyl ethyl ketone for use in the reactions. All other chemicals were purified and dried as necessary (Table 1). Sheet molds were made of polypropylene, block molds were made of Teflon.

Polymer blends were made according to the following general procedure for two step polymerization (Fig. 6): PTMO of the selected molecular weight (Table 2) was melted and poured into a three-necked round-bottom flask and stirred at 100°C for two hours under vacuum to remove water and dissolved gases. A predetermined number (Table 2) of equivalents (with a 5% excess) of p-TMXDI was added to make a prepolymer reaction mixture weighing 250-350 grams (for multiple samples; 150 grams for single blocks). (The NCO:OH ratio of 1.05:1.00 is useful for: 1. scavenging residual moisture and 2. producing some crosslinking by allophanate bonds.) DBTDL catalyst solution was added (150-350 ul for 0.002-0.005% by weight of catalyst) and the resulting prepolymer mixture was stirred under vacuum at 100°C for two hours. Multiple sample mixtures were divided into 50 gram aliquots in plastic cups and refrigerated under vacuum, then melted under vacuum at 100°C individually as needed. After cooling to about 60°C the prepolymer was stirred while the appropriate number (Table 2) of equivalents of chain extender and crosslinker (premelted as necessary) were added, and stirring was con-
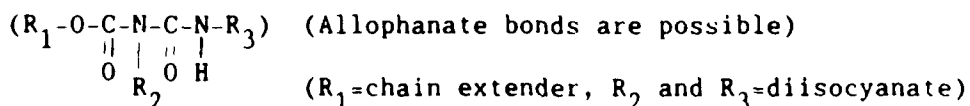
tinued for 45 seconds. The mixture was degassed for 30-45 seconds under vacuum, then poured (1 atm.) into an appropriate mold (12.7cm x 12.7cm x 1.4mm for sheets, 6.4cm x 6.4cm x 1.9cm for blocks). The sheet molds were pressed at 1.03 MPa (150 psi) and $100^{o}C$ for 1 hour, then oven-cured at $100^{o}C$ for 16-18 hours (1 atm.); the block molds were covered with Teflon and oven-cured under nitrogen gas for 16-18 hours at $100^{o}C$. The samples were aged at room temperature for two weeks before testing.

The model compounds (Fig. 7) were made as follows: p-TMXDI (5 grams) was refluxed in 75 ml of methanol, and another 5 grams separately in 75 ml of absolute ethanol, for 2 hours in the presence of 5 drops of triethylamine which was used as catalyst; crystals were allowed to grow at room temperature from the evaporating solvents.

Table 1. Chemical Sources

Chemical	Source	Grade or Purity
PTMO	duPont	
BD	Aldrich	99+%
EG	Aldrich	99+%
HD	Aldrich	99+%
TMP	Aldrich	
TEA	Aldrich	97%
HER	ICN Pharmaceuticals	
HEB	Akzo Chemie Nederland bv	
DBTDL	M&T Chemicals	
p-TMXDI	American Cyanamid	

26

Figure 6. Typical Preparation[a]

$$p\text{-TMXDI} \quad + \quad \text{PTMO}$$

$$\downarrow \quad 100^{\circ}\text{C}, \text{Cat.}$$

$$p\text{-TMXDI} \quad + \quad \text{OCN} - \overset{\underset{|}{\text{CH}_3}}{\underset{\underset{|}{\text{CH}_3}}{\text{C}}} \underset{}{\underset{}{\bigcirc}} \overset{\underset{|}{\text{CH}_3}}{\underset{\underset{|}{\text{CH}_3}}{\text{C}}} - \overset{}{\underset{\underset{\text{H}}{|}}{\text{N}}} - \overset{\overset{\text{O}}{\|}}{\text{C}} - \text{O} - [(\text{CH}_2)_4 - \text{O}-]_n - \overset{\overset{\text{O}}{\|}}{\text{C}} - \overset{}{\underset{\underset{\text{H}}{|}}{\text{N}}} - \overset{\underset{|}{\text{CH}_3}}{\underset{\underset{|}{\text{CH}_3}}{\text{C}}} \underset{}{\underset{}{\bigcirc}} \overset{\underset{|}{\text{CH}_3}}{\underset{\underset{|}{\text{CH}_3}}{\text{C}}} - \text{NCO}$$

$$\downarrow \quad \text{BD}, 100^{\circ}\text{C}$$

$$\left[-\text{O}-[(\text{CH}_2)_4\text{O}]_n \overset{\overset{\text{H}}{|}}{\underset{\underset{\text{O}}{\|}}{\text{C}}} - \text{N} - \overset{\underset{|}{\text{CH}_3}}{\underset{\underset{|}{\text{CH}_3}}{\text{C}}} \underset{}{\underset{}{\bigcirc}} \overset{\underset{|}{\text{CH}_3}}{\underset{\underset{|}{\text{CH}_3}}{\text{C}}} - \text{N} - \overset{\overset{\text{O}}{\|}}{\underset{\underset{\text{H}}{|}}{\text{C}}} - [\text{O} - (\text{CH}_2)_4\text{O} - \overset{}{\underset{\underset{\text{O}}{\|}}{\text{C}}} - \overset{\overset{\text{H}}{|}}{\text{N}} - \overset{\underset{|}{\text{CH}_3}}{\underset{\underset{|}{\text{CH}_3}}{\text{C}}} \underset{}{\underset{}{\bigcirc}} \overset{\underset{|}{\text{CH}_3}}{\underset{\underset{|}{\text{CH}_3}}{\text{C}}} - \text{N} - \overset{\overset{\text{O}}{\|}}{\underset{\underset{\text{H}}{|}}{\text{C}}} -]_x \right]_y$$

$(R_1\text{-O-}\overset{\overset{}{\|}}{\underset{\text{O}}{\text{C}}}\text{-}\overset{}{\underset{R_2}{\text{N}}}\text{-}\overset{\overset{}{\|}}{\underset{\text{O}}{\text{C}}}\text{-}\overset{}{\underset{\text{H}}{\text{N}}}\text{-}R_3)$ (Allophanate bonds are possible)

(R_1=chain extender, R_2 and R_3=diisocyanate)
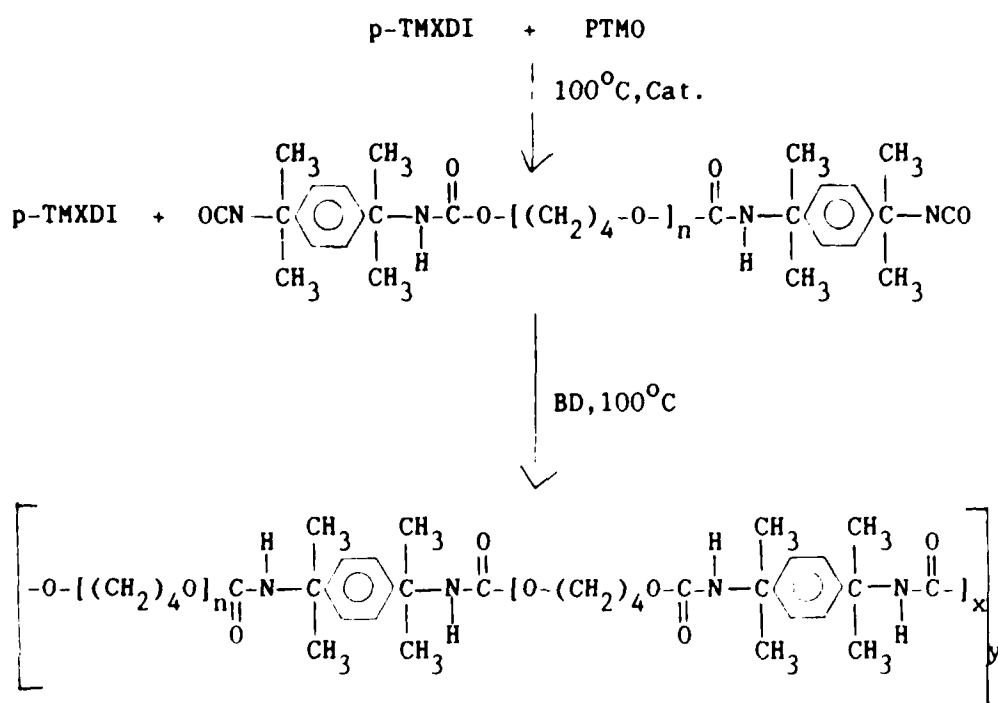
x=between 0 and 9

y=a repeat which produces mol.wt. $\approx$5,000 to 50,000

[a]Some percentage of p-TMXDI may react on both NCO's in the first step to form a higher molecular weight prepolymer; there is even a small chance that one PTMO and one p-TMXDI may form a ring. These possibilities are dependent upon ratios of equivalents and other factors such as effects of mechanical mixing. The chains may terminate with PTMO or chain extender hydroxyls or unreacted isocyanates.

Table 2. Compounding Equivalent Ratios[a]

Ident. no.[bc]	PTMO[d]	TMXDI[e]	Chain extender[f]	Crosslinker[f]	%HS[g]
2-25-0	1934	2.625	1.5(BD)		29
2-25-20P	1934	2.625	1.2(BD)	0.2(TMP)	29
2-25-50-50	1934	2.625	.75(BD).75(EG)		27
3-50-25P	2695	5.25	3.0(BD)	0.67(TMP)	38
3-50-0-H	2695	5.25	4.0(HD)		39
3-50-0-R	2695	5.25	4.0(HER)		43
3-50-25P-R	2695	5.25	3.0(HER)	0.67(TMP)	42
3-50-7P-R	2695	5.25	3.72(HER)	0.187(TMP)	43
2-40-0-R	1934	4.20	3.0(HER)		46
2-40-0-B	1934	4.20	3.0(HEB)		51
3-77-0-R	2695	8.07	6.73(HER)		55
3-77-0-B	2695	8.07	6.73(HEB)		60
3-70-7A-B	2695	7.35	5.58(HEB)	0.28(TEA)	57
3-70-7A-R	2695	7.35	5.58(HER)	0.28(TEA)	52
3-70-0	2695	7.35	6.0(BD)		46
3-70-7A	2695	7.35	5.58(BD)	0.28(TEA)	46
3-70-15A	2695	7.35	5.10(BD)	0.60(TEA)	47
3-60-0	2695	6.30	5.0(BD)		42
3-60-7A	2695	6.30	4.65(BD)	0.23(TEA)	42
3-60-15A	2695	6.30	4.25(BD)	0.50(TEA)	43
3-50-0	2695	5.25	4.0(BD)		38
3-50-7A	2695	5.25	3.72(BD)	0.19(TEA)	38
3-50-15A	2695	5.25	3.40(BD)	0.40(TEA)	38
3-40-0	2695	4.20	3.0(BD)		32
3-40-7A	2695	4.20	2.78(BD)	0.14(TEA)	32
3-40-15A	2695	4.20	2.55(BD)	0.30(TEA)	33
2-25-7A	1934	2.625	1.40(BD)	0.07(TEA)	29
2-30-7A	1934	3.15	1.86(BD)	0.093(TEA)	33
2-40-7A	1934	4.20	2.79(BD)	0.14(TEA)	40
2-50-7A	1934	5.25	3.72(BD)	0.187(TEA)	46
3-25-7A	2695	2.625	1.40(BD)	0.07(TEA)	22
3-30-7A	2695	3.15	1.86(BD)	0.093(TEA)	26
3-35-7A	2695	3.675	2.33(BD)	0.12(TEA)	29
3-45-7A	2695	4.725	3.26(BD)	0.16(TEA)	35

footnotes on next page

Compounding Ratio Footnotes (for Table 2)

[a]1 equivalent is the number of molar equivalents (i.e., PTMO, BD, p-TMXDI, etc., have two reactive ends while TMP and TEA have three, but each, except for PTMO, is listed in the table according to the number of moles (molecules), not the ratio of reactive ends).

if 1 equiv   PTMO = 2 mole -OH

then 1 equiv p-TMXDI = 2 mole -NCO

and 1 equiv   BD = 2 mole -OH

and 1 equiv   TEA = 3 mole -OH

2-25-50-50 = PTMO 1934-2.5 equiv. TMXDI-50%BD-50%EG

3-50-25P-R = PTMO 2695-5.0 equiv. TMXDI-25%TMP-75%HER

3-70-7A-B = PTMO 2695-7.0 equiv. TMXDI-7%TEA-93%HEB

3-50-7A   = PTMO 2695-5.0 equiv. TMXDI-7%TEA-93%BD

[b]In general the Ident.no. refers to: 1. PTMO mol.wt. (2=1934,3=2695)

2. TMXDI equiv. (e.g. 25=2.5)

1-2-3-4   3. % of crosslinker (except BD/EG)

4. chain extender (BD unmarked)

[c]For Ident.no.: P=TMP%, A=TEA% (crosslinker), percent of chain extender replaced by crosslinker; H=HD, R=HER, B=HEB (chain extender).

[d]PTMO data refers to mol.wt. Number of equivalents is always 1.0.

[e](no. of moles)

[f]Chain extender and crosslinker used are in parentheses (no. of moles).

[g] % Hard Segment.

Figure 7. Model Compounds of p-TMXDI.

MeTMXMe

EtTMXEt
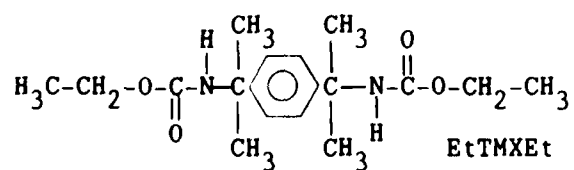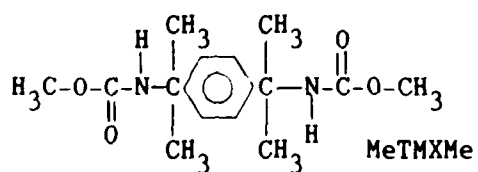
B. Macroscopic Physical and Spectral Properties

Tensile tests were run on an Instron model 1120 (100 Kg cell). The dumbell-shaped microdie samples were drawn apart at 200 mm/min while force and elongation were measured. Tear tests were run using die-cut trouser-shaped samples on the same instrument at the same rate. The maximum force needed to tear the sample was recorded. Tensile testing was run according to ASTM D 1708 and tear testing followed ASTM D 470 (American Society for Testing and Materials).

DSC tests were recorded on a Perkin Elmer DSC2 equipped with a 3600 TADS (Thermal Analysis Data Station computer). Samples weighing 10-15 mg were sealed in either aluminum or steel pans and placed in a platinum alloy cell mounted in an aluminum block. An empty reference pan of similar weight was placed in an adjacent cell. (A background scan with empty cells was run for later subtraction when the baseline was not sufficiently flat.) Scans were run (normally at 20°/min) from 150 to 300 K (-123 to 27°C) and from 300 to 500 K (27 to 227°C) or higher. Peaks and transitions were analyzed by manually defining the beginning and end points and instructing the software to calculate the resulting parameters (peak temperature, midpoint, etc.)

TMA (thermomechanical analysis) was run using a Perkin Elmer TMS-1 with a strip chart recorder to graph probe displacement with respect to increasing temperature. The sample holder was a quartz tube with a flat bottom, and the probe was a quartz rod with a flat circular end 1 mm in diameter, supported at the other end by a neutral buoyancy oil reservoir. The force was provided by a weight pan, normally holding 20

grams, attached directly to the probe assembly. A small sample (thickness 1.25-2.50 mm) was placed in the sample holder which was cooled to 150 K before lowering the probe (helium purge). The sample chamber was then heated at 20°/min until sample failure (probe penetration; maximum temperature is 550 K). A diagram of the TMA apparatus is displayed in Figure 8.

TGA (thermogravimetric analysis) was run using a Perkin Elmer TGS-2. A sample weighing 5-10 mg was placed in the sample pan. The weight was monitored as the sample was heated from room temperature at 10°/min until the entire sample was evaporated. This experiment was run in both nitrogen and standard air atmospheres.

FTIR spectra were run on two different instruments. One was a Perkin Elmer 1550 interfaced with a Perkin Elmer 7500 computer. The other was a Mattson Cygnus 25 FTIR coupled to a Mattson Starlab computer. Attenuated total reflectance spectra were run on the polymers, and KBr disks were used for the model compounds.

Hysteresis testing of the blocks was run on an Instron 1322 servo-hydraulic test machine. A temperature probe in the center of the blocks monitored temperature rise during the test. The blocks were cycled between 500 KPa and 5 MPa (72 to 720 psi) at 20 Hz for a total of 200,000 cycles. Data was acquired on load and stroke measurements by a Nicolet digital oscilloscope. This data, plus temperature, was recorded on a floppy disk for later analysis.

WAXS patterns were collected using a one dimensional multichannel analyzer programmed to record 1000 channels on a LeCroy computer and store data on a floppy disk. The effective 2θ detector range was from

32

$\sim$5° to $\sim$29.5°. The sheet sample ($\sim$1.4mm thick) was held in a four circle goniometer and irradiated with nickel-filtered CuKα (1.54$\mathring{A}$) X-rays for 6 hours. Sample to detector distance was 22cm.

Figure 8. TMA Apparatus.

WEIGHT TRAY

FLOAT SUSPENSION

LVDT

LVDT CORE

GAS PURGE

PROBE COUPLING

SAMPLE TUBE

FURNACE

HEAT SINK

INSULATION

COOLANT
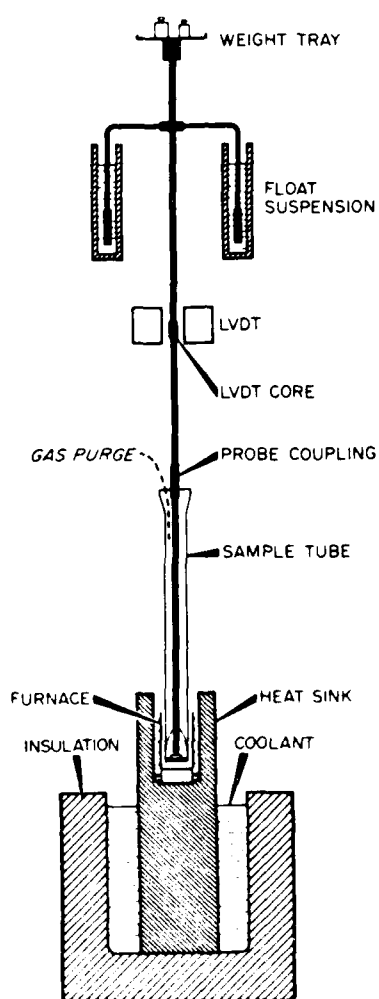
V. EXPERIMENTAL RESULTS

A. Mechanical Testing

Table 3 shows the results of mechanical tests on samples which were 1.4mm thick and cut to the dimensions shown in Figure 9. General observations can be made on this data. For the 100% modulus (100%(MPa)) results, the samples extended by BD showed better strength than most of the HER and HEB extended samples. However, for the 300% modulus (300%(MPa)) and the ultimate tensile strength (Str.(MPa)) the results are not uniform: some of the BD-extended samples developed cracks during elongation, possibly due to some crystallization caused by extension. (The HER-extended samples were observed to be softer materials than the other samples.) The maximum elongation at break also showed better tensile properties for those samples extended with HER or HEB. For the tear test, most of the BD samples are clearly superior and show an increase in tear strength as the amount of crosslinker (TEA) is increased. This is illustrated in Figures 10-12, which display comparisons of mechanical data for the last 12 samples in Table 3. In summary, the BD samples have better tear strength and better tensile strength for moderate elongation.

B. Thermal Behavior

Table 4 has the DSC results on sheet samples. The soft segments all

35

Table 3. Tensile/Tear Tests[a]

Ident. no.	100%(MPa)	300%(MPa)	Str.(MPa)	Elong(%)	Tear(kN/m)
3-50-0-R	3.93	7.86	29.8	590	9.1
3-50-25P-R	4.34	7.21	23.8	450	4.6
3-50-7P-R	3.45	9.72	24.1	610	6.0
2-40-0-R	2.69	3.69	14.8	710	4.9
2-40-0-B	2.96	4.24	13.3	650	5.7
3-77-0-B	9.45	11.2	15.6	425	8.7
3-70-7A-B	7.58	9.93	17.7	475	9.1
3-70-7A-R	3.72	8.65	12.5	510	6.3
3-70-0	12.4		14.2	220	20.7
3-70-7A	11.4	16.0	17.7	385	15.4
3-70-15A	10.5	16.5	24.0	410	20.1
3-60-0	10.4		10.4	100	9.6
3-60-7A	10.3	15.2	16.2	350	15.8
3-60-15A	8.86		9.83	160	18.4
3-50-0	8.03		8.45	115	7.5
3-50-7A	6.03		6.24	120	13.0
3-50-15A	7.48	11.2	15.1	430	24.5
3-40-0	6.90		8.27	265	11.6
3-40-7A	6.69	9.93	12.5	450	23.8
3-40-15A	6.21	9.10	16.8	565	25.9

100%=force to give twice original length;   300%=force to give 4 times original length;   Str.=force required to break;   Elong=% elongation at break (% extended from original length);   Tear=force to tear (force/ elongation to tear)

[a] 4 samples run for each test (values are average with 10% error).

Figure 9. Tensile and Tear Die Dimensions (mm).
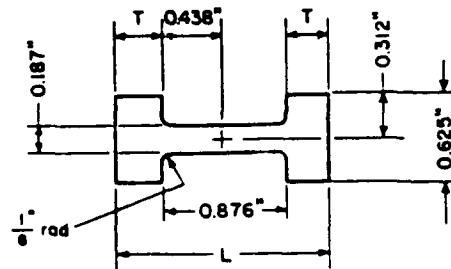
Tensile

ASTM D 1708

Tolerance: ±0.051 mm (±0.002 in.)
Thickness = thickness of sheet.
Minimum tab length. T = 7.9 mm (0.312 in.) (Larger tabs shall be used wherever possible.)
Minimum length. L = 38.1 mm (1.50 in.)

Table of Metric Equivalents

in	mm
⅛	3.2
0.187	4.75
0.438	11.13
0.312	7.92
0.625	15.88
0.876	22.25
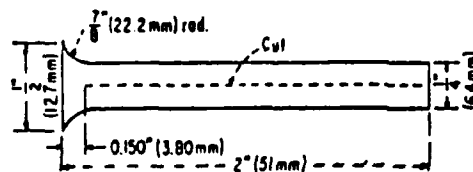
Tear

ASTM D 470

Figure 10. Comparison of Tensile Strength.

37
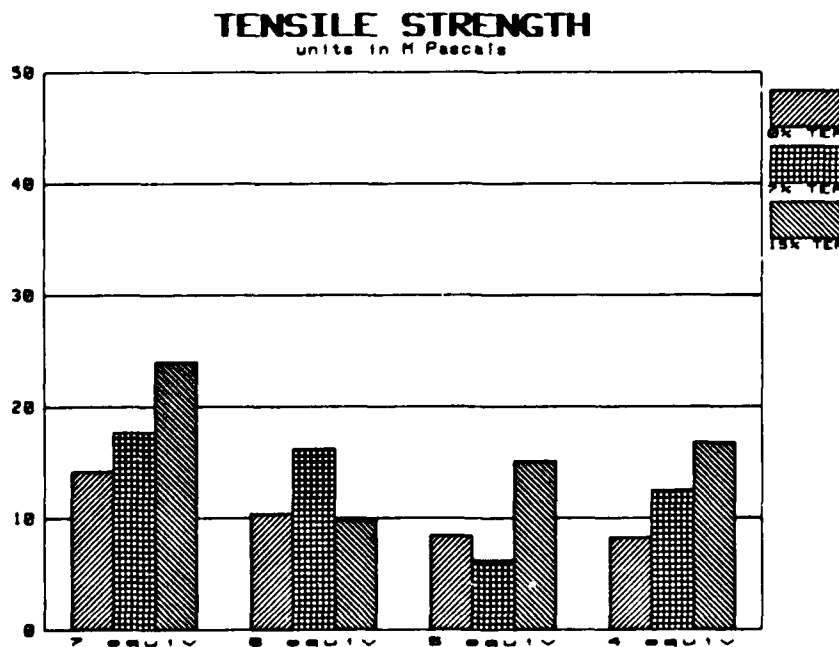
Figure 11. Comparison of Elongation.

ELONGATION
units in Percent
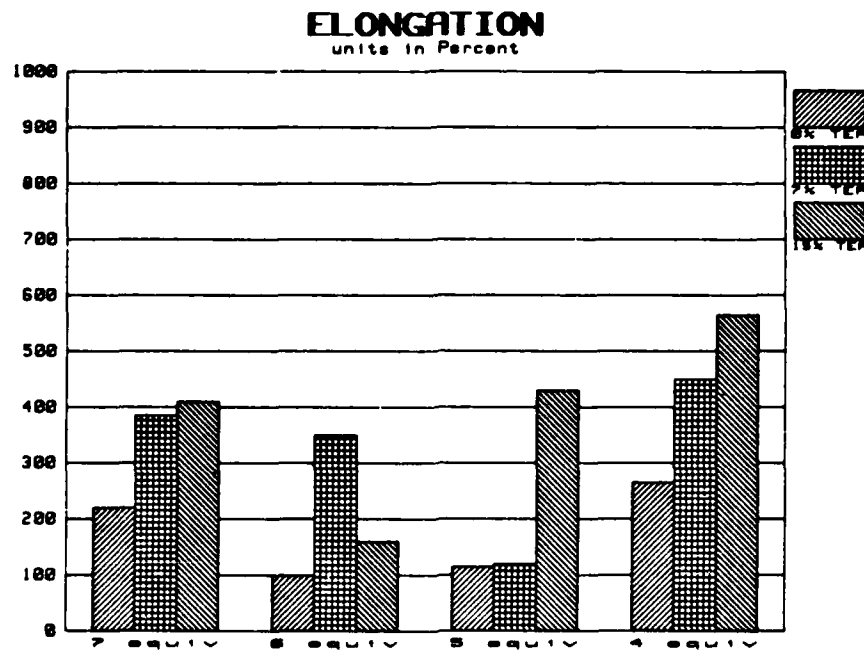
Figure 12. Comparison of Tear Strength.

TEAR STRENGTH
units in k Newtons/meter
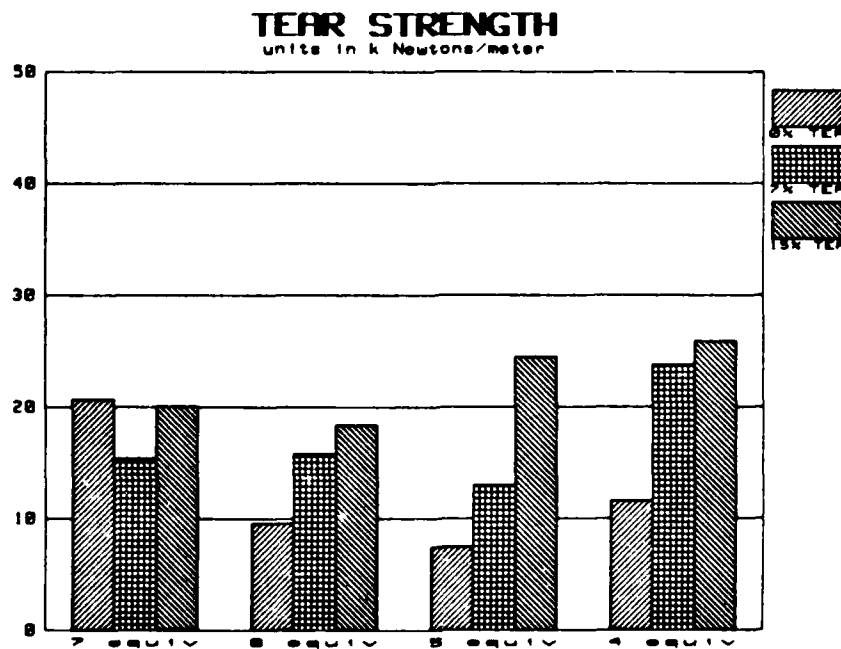
Table 4. DSC Results (^{o}C)

Ident. no.	Soft segment T_g	Hard segment T_m (ΔH,joules/gram)
2-25-0	-80	168(.63),180(3.39),190(.42)
2-25-20P	-77	138(2.51),164(.59),181(.96)
2-25-50-50	-76	170(.13),180(.63)
3-50-25P	-81.5	159.5(17.49),170(4.39)
3-50-0-H	-82.5	135.5(8.49)
3-50-0-R	-79	185.5(2.72)
3-50-25P-R	-79	255(5.15)
3-50-7P-R	-78.5	208.5(2.22),223(1.51)
3-70-0	-84.5	199.0, 215.5 (29.92 combined)
3-70-7A	-83	194.5(23.14)
3-70-15A	-83	188(13.97),259(2.18)
3-60-0	-81.5	190(4.64),217(11.76)
3-60-7A	-81	183((7.20),207(3.93),232.5(1.09)
3-60-15A	-83	183(19.5)
3-50-0	-83	179(5.31),217(15.36)
3-50-7A	-84	178.5(3.56),203(7.99)
3-50-15A	-82	182(11.46)
3-40-0	-78	176(3.93),213(9.33)
3-40-7A	-82	179.5(12.34)
3-40-15A	-79	176.5(9.67)

(values are average with $\pm 1^{o}$C error, runs repeatable to $\pm$ 5°C)

show a T_g of $\approx -80^{o}C$. Most of the hard segments have a T_m of $>150^{o}C$ as the first melting transition, with additional T_m's at higher temperature, indicating the possible existence of different degrees of crystallinity or different lengths of hard segment chains. Figure 13 displays a comparison of the first DSC melting transitions for the last 12 samples in Table 4. The thermal energy (joules/gram) needed to melt these regions is also some indication of the degree of crystallinity. Figure 14 compares the total enthalpy for the last 12 samples in Table 4. Most samples containing BD required energy (total) of >10 joules/gram for the transitions while most samples with HER, HEB, or HD needed ~5 joules/gram or less.

The TMA results (Table 5) are more indicative of a major difference between chain extension by BD and chain extension by HER and HEB. The BD-extended samples soften above $150^{o}C$ in almost all cases. The other chain extenders produce samples with softening ranges which are not suitable for materials which may be subjected to high internal temperatures (up to ~$100^{o}C$). Only those HER or HEB samples with some cross-linker content (e.g., ident no. 3-50-25P-R) resisted thermal softening until ~$150^{o}C$. A minor trend is noted in the BD samples crosslinked by TEA. The softening temperature shows a slight decrease on the repeat runs for crosslinked samples, while the corresponding linear (uncross-linked) samples show a slight increase. Figure 15 compares first-run data for the last 12 samples in Table 5. This may be an indication of the linear samples forming more ordered hard segment regions after the first softening transition (which would permit realignment of chains).

40

Table 5. TMA Results ($^{\circ}$C)[a]

Ident. no.	First Run (final softening)	Repeat Run (same sample)
2-25-0	153	155
2-25-20P	152	147
2-25-50-50	72	81
3-50-25P	158	153
3-50-0-R	60	45
3-50-25P-R	195	192
3-50-7P-R	152	153
2-40-0-R	63	15
2-40-0-B	67	22
3-77-0-R	53	43
3-77-0-B	57	50
3-70-7A-B	55	50
3-70-7A-R	61	15
3-70-0	198	202
3-70-7A	191	171
3-70-15A	182	181
3-60-0	188	190
3-60-7A	182	180
3-60-15A	177	166
3-50-0	186	192
3-50-7A	176	172
3-50-15A	178	171
3-40-0	177	186
3-40-7A	176	171
3-40-15A	171	158

[a]sheet samples

41

Figure 13. Comparison of DSC Temperature.

DSC HARD SEGMENT MELT
units in Centigrade
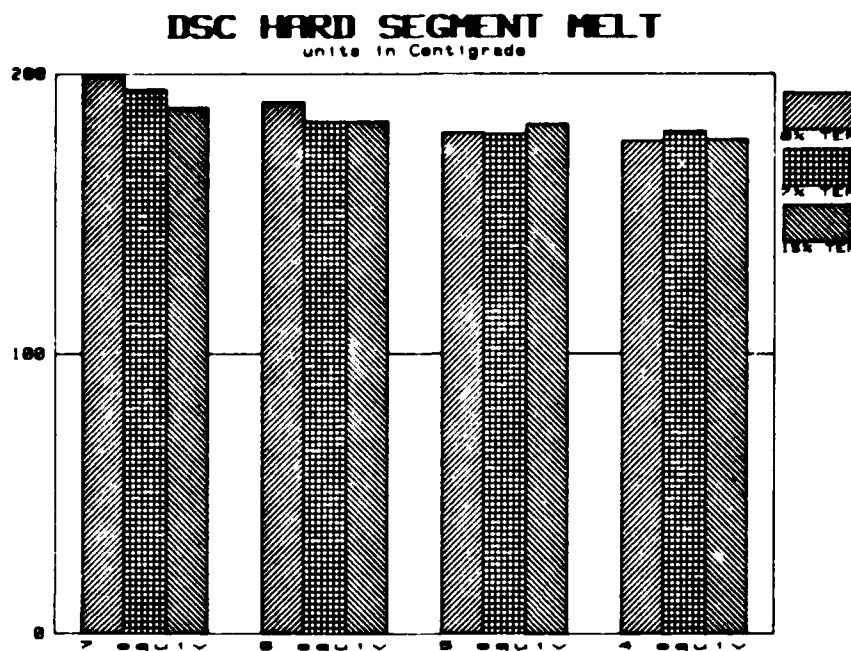
Figure 14. Comparison of DSC Enthalpy.

DSC MELTING ENTHALPY (TOTAL)
units in joules/gram
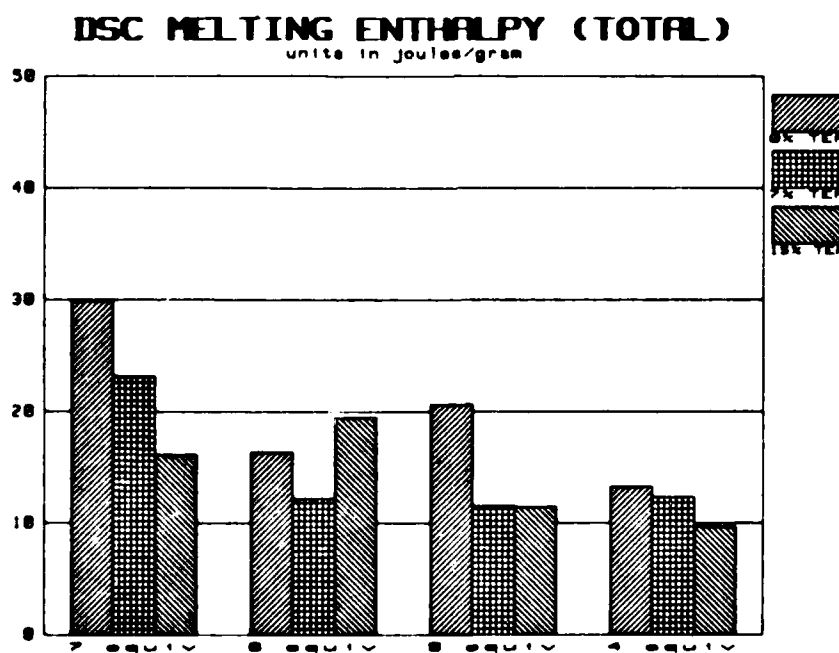
Figure 15. Comparison of TMA Melting.

43
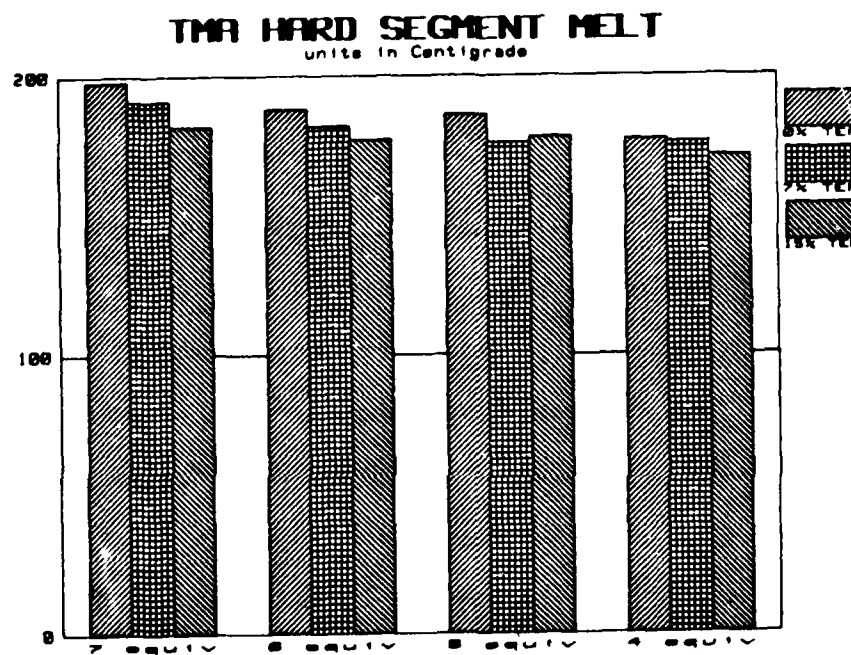
Figure 16 shows a typical TMA sample run for 2-25-7A.

The block samples were also subjected to DSC and TMA analysis (Table 6). As noted before, the sheets were initially cured in closed molds under pressure while the blocks were allowed to cure at ambient pressure (1 atm.) while still liquid. This has produced some differences in thermal behavior between sheets and blocks. The blocks consistently show two separate melting transitions, the second occuring above 200°C. The immediate rescan (by DSC) of some samples apparently allows little time for reforming crystalline regions, since the joules/gram value is reduced compared to the original scan. The high scan temperature (up to 277°C on DSC) may also disrupt some covalent urethane bonds. Remeasurement of some samples after annealing gave results similar to those obtained originally. Figures 17 and 18 display, respectively, the low and high temperature DSC scans for sample 2-50-7A.

TGA (Fig. 19) shows the thermal decomposition of a polyurethane sample (ident no. 3-70-15A) in both air and nitrogen atmospheres. Decomposition does not occur until ~250°C and is essentially complete at ~425°C. No residual charred material was present after the test, although aromatic materials (such as styrene-butadiene rubber with carbon black) often leave chars.

C. Infrared Spectroscopy

The characteristic absorptions of polyurethanes reported in the literature[64] are compared with those of p-TMXDI polyurethanes (Table 7).

44

Figure 16. TMA Scan for 2-25-7A.
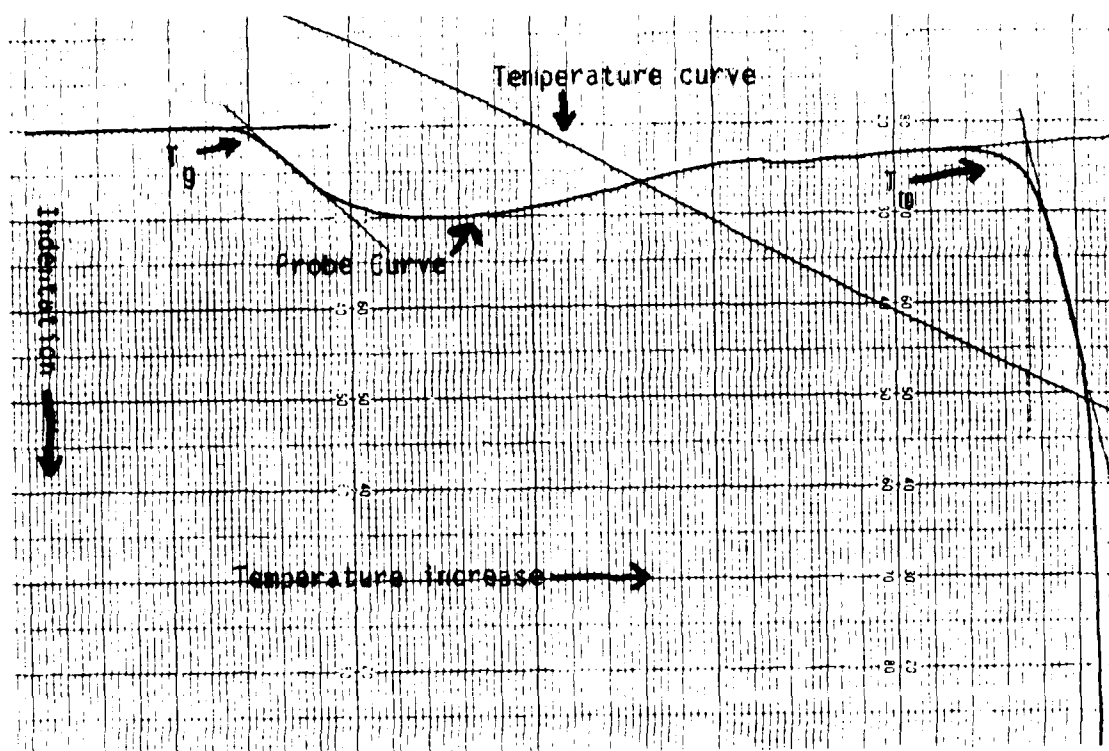
Table 6. DSC and TMA on Blocks ($^{\circ}$C)

Table 6A. DSC on samples which were immediately rescanned.

Ident No.	T_{m1}	T_{m2}	joules/g(total)	T_m(rescan)[a]	joules/g(rescan)[a]
3-40-7A	183	212	20.13	186	3.64
3-50-7A	186	212	17.24	193	8.87
3-60-7A	187	217	25.36	195	7.78
3-70-7A	189	215	27.03	200	12.76

Table 6B. DSC and TMA on samples scanned only once.

Ident No.	T_{m1}	T_{m2}	joules/g(total)	T_c(joules/gram)[b]	TMA T_m
2-25-7A	153	219	10.36	184(-4.94)	137
2-30-7A	167	211	20.45		157
2-40-7A	171	222	19.33		157
2-50-7A	168	201	15.10		165
3-25-7A	164	223	12.05	187(-3.31)	160
3-30-7A	172	203	9.96		165
3-35-7A	165	224	11.17	192(-3.51)	165
3-45-7A	168	205	8.71		169

Table 6C. TMA and DSC on samples which were annealed.

Ident No.	TMA T_m[c]	TMA T_m[d]	T_{m1}[d]	T_{m2}[d]	joules/g(total)[d]
3-40-7A	170	168	183	210	21.97
3-50-7A	173	177	191	216	23.97
3-60-7A	175	168	194	218	24.02
3-70-7A	172	175	188	216	29.46

[a] for rescan, sample was immediately cooled (80°C/min) to 300 K (27°C) after first scan.

[b] crystallization (T_c) was noted in some samples after the first melt (T_{m1}).

[c] before annealing

[d] annealed at 150°C for 4 hours and stored at room temperature for 2 weeks before scan.

Figure 17. Low Temperature DSC for 2-50-7A.

TMX-507-1

WT: 17.82 mg

SCAN RATE: 20.89 deg/min

T/G FROM: 178.74
TO: 201.88
ONSET: 184.79
CAL/GDEG: 5.85582E-82
MIDPOINT: 189.35

PEAK FROM: 213.43
TO: 253.44
ONSET: 217.96
CAL/GRAM: -1.27
PEAK FROM: 262.18
TO: 289.97
ONSET: 265.87
CAL/GRAM: 1.48

MAX: 278.48

MIN: 233.58

ENDO>

MCAL/SEC

TEMPERATURE (K)

DSC

B.Z.   FILE: TM587.DA

DATE: 86/82/84   TIME: 13:56
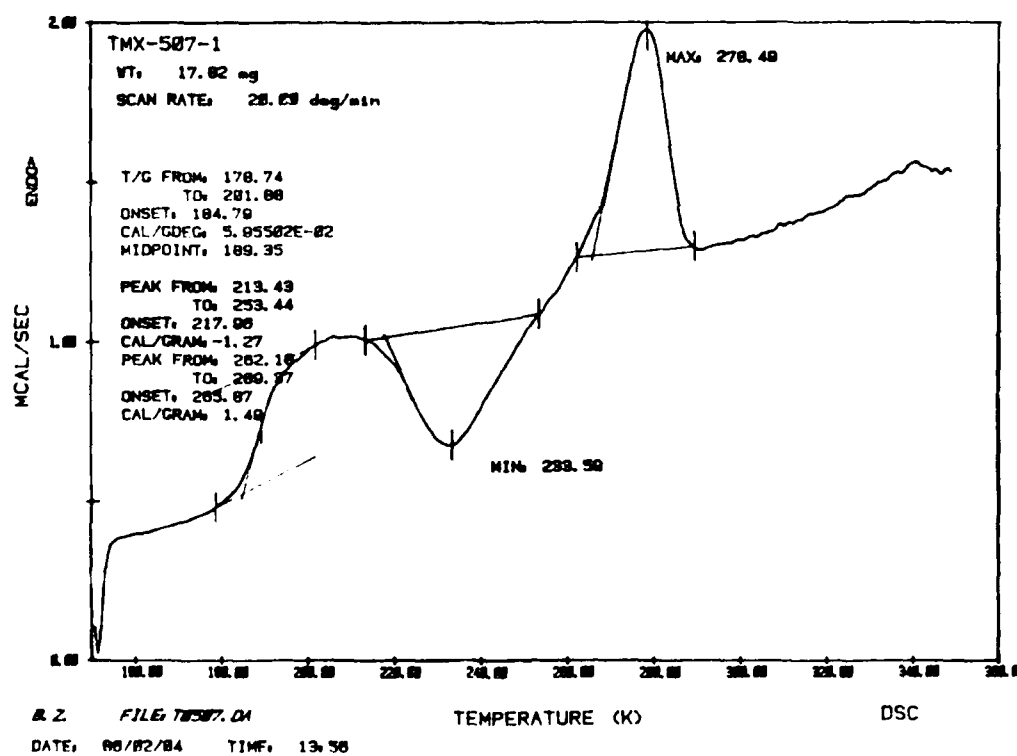
Figure 18. High Temperature DSC for 2-50-7A.

TMX-2-507-1

WT: 42.15 mg

SCAN RATE: 20.88 deg/min

PEAK FROM: 415.22
TO: 458.2
ONSET: 424.14
CAL/GRAM: 2.12

PEAK FROM: 458.18
TO: 581.17
ONSET: 462.69
CAL/GRAM: 1.48

MAX: 441.53 MAX: 474.31

ENDO>

MCAL/SEC

TEMPERATURE (K)

DSC

B.Z.   FILE: Z2587.DA

DATE: 86/89/83   TIME: 88.88

47
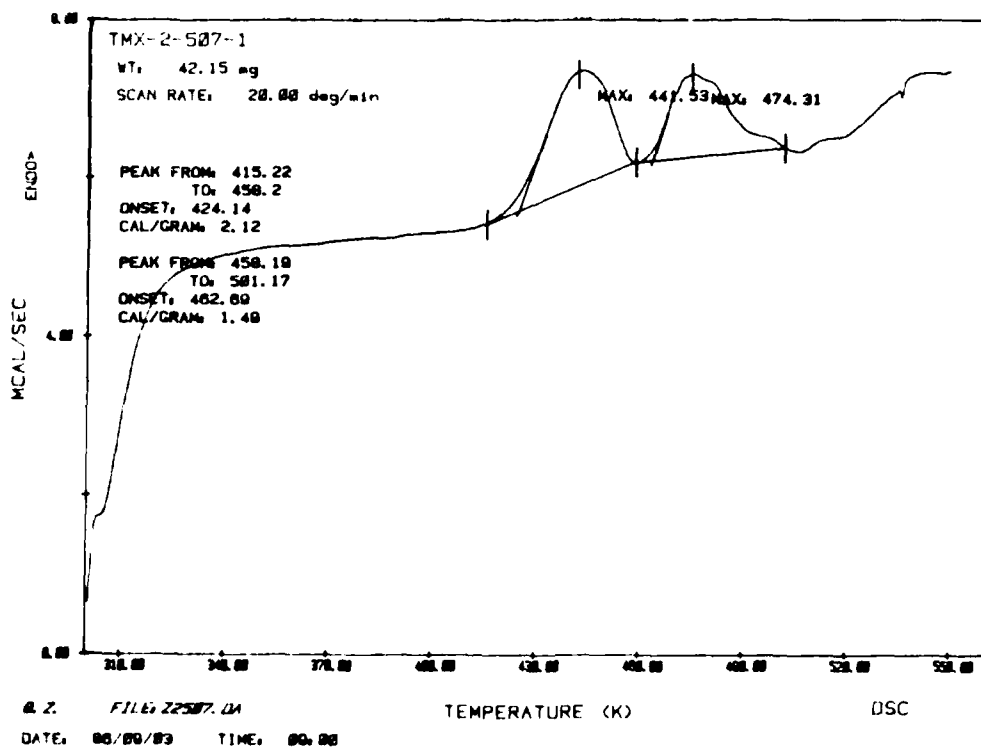
Figure 19. TGA of 3-70-15A in Air and Nitrogen.
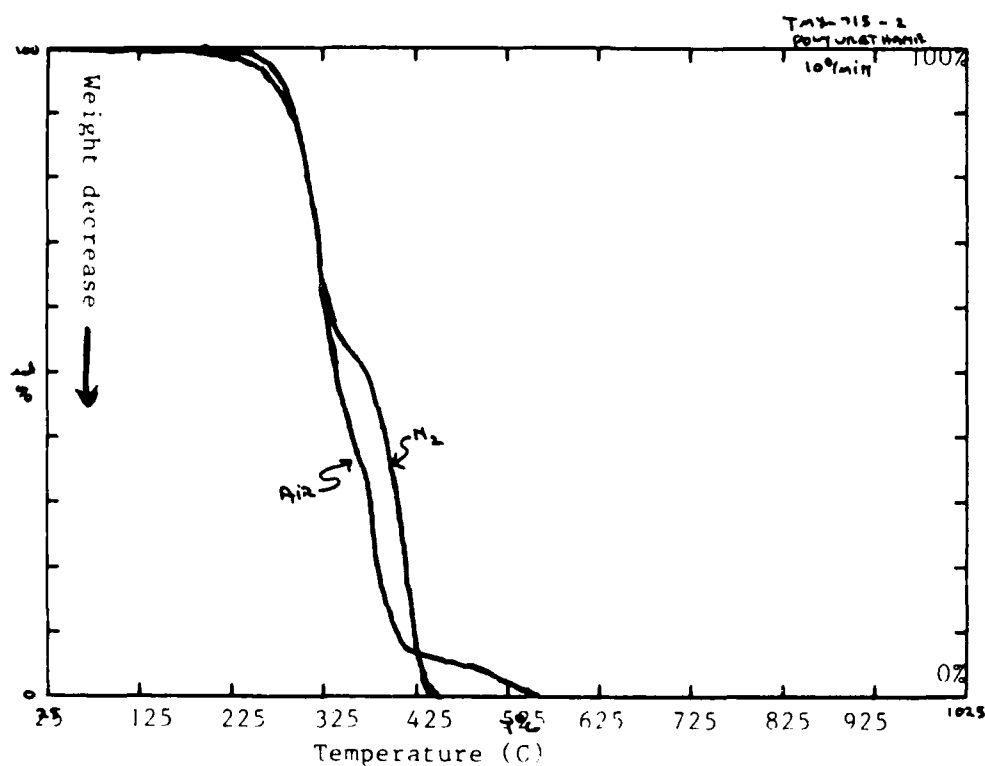
Table 7. Infrared Absorbances

Frequency (cm^{-1})

Vibrational assignment	Ref. 64	Et-TMX-Et	3-60-7A
N-H stretch (free)	3444,3384		
N-H stretch (bonded) carbonyl	3328	3328	3328,3338
" " " ether	3262		
Carbonyl stretch (free)	1730	1723	1723
" " (H-bonded)	1704	1699	1699
Amide III (C-N stretch + N-H bend)	1534	1533,1539	1533,1539
Amide IV " " " "	1311		
Amide V " " " "	1229		
C-O-C stretch of (C=O)-O-C	1081	1082,1095	1082,1095
Out of plane -(C=O)-O- bend	772	781	781

48

Two characteristic types of spectra were recorded. All BD-extended samples gave essentially identical scans, with strong N-H absorbances and carbonyls with small "free" C=O shoulders (non-hydrogen bonded) (Fig. 20). The samples with HER or HEB as chain extender were also similar in their own class, but with weaker N-H absorbances and the "free" carbonyl peak showing a relatively equal intensity compared to the hydrogen-bonded C=O stretch (Fig. 21). This provides some indication that HER and HEB inhibit the proper alignment of some chains which is necessary for hydrogen bonding (and perhaps crystallization).

D. Hysteresis Results

Compressive fatigue tests were performed on block samples of the polyurethane blends (Table 8) (Fig. 22). The samples survived testing without any visible damage, except for sample 3-25-7A which contained the lowest percentage of hard segment in the blocks which were prepared. The hardness was essentially unchanged by the test (softening of the sample usually results in increased hysteretic heatup, which was experienced by sample 3-25-7A. Figure 23 shows the testing method for hardness (ASTM D 2240).

E. Model Compound Characterization

Spectral data was collected for Me-TMX-Me (the melting point was $189^{o}C$ by DSC). Figure 24 shows the FTIR scan with the characteristic
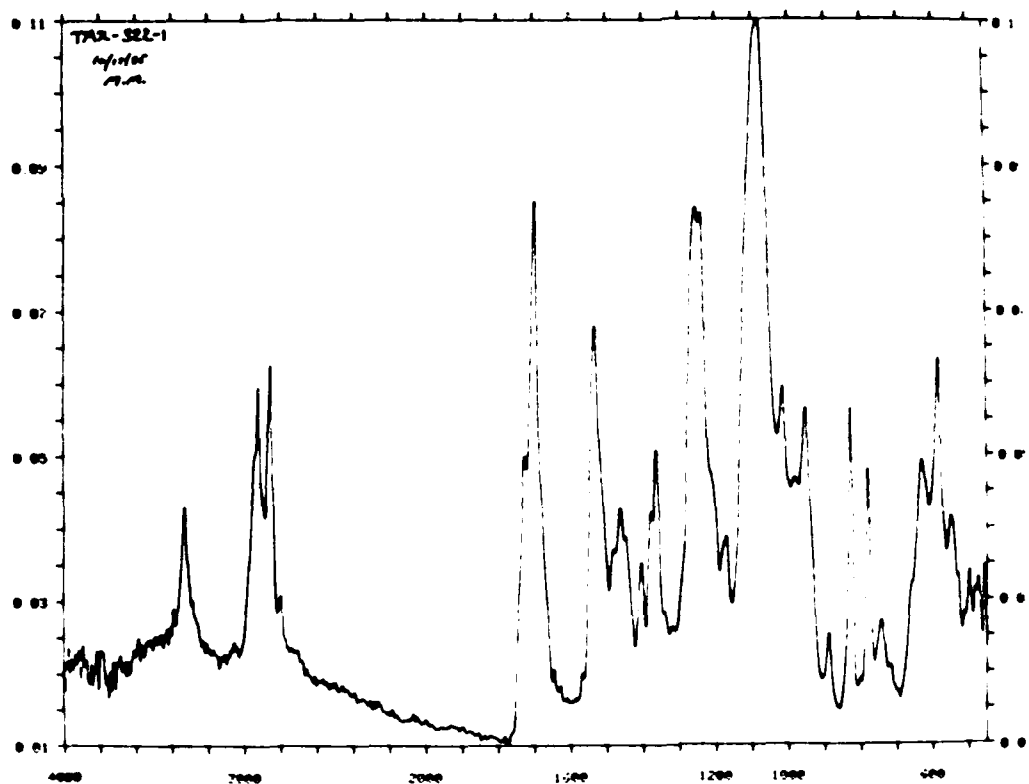
Figure 20. FTIR
of 3-70-7A.
(Perkin Elmer)
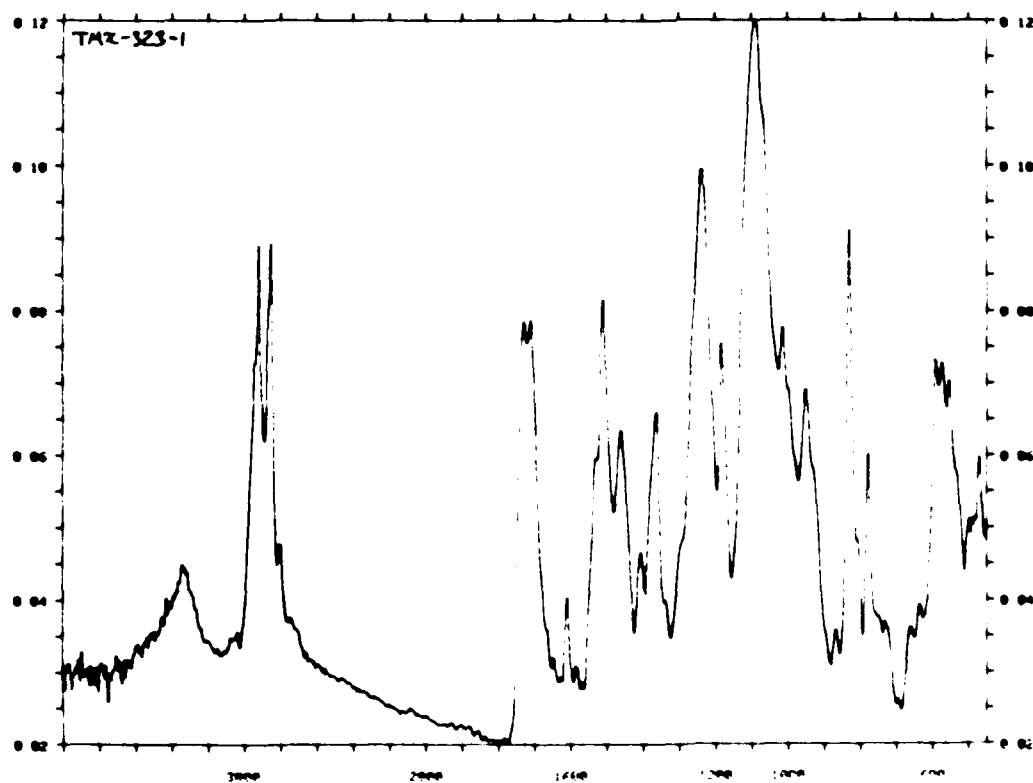
Figure 21. FTIR
of 3-70-7A-B.
(Perkin Elmer)

Table 8. Compressive Fatigue Tests ($^{\circ}$C)[a]

Ident No.	1K	2.5K	5K	10K	20K	50K	100K	150K	200K
2-25-7A	32.2	36.1	42.2	44.4	50.0	56.1	59.4	61.1	61.1
2-30-7A	25.0	28.9	31.7	36.7	40.0	42.2	43.9	----	44.4
2-40-7A	29.4	33.3	36.7	40.6	43.3	46.1	47.8	47.2	47.2
2-50-7A	22.8	26.1	28.3	31.7	35.0	37.8	38.9	38.9	40.0
3-25-7A	36.1	46.7	77.2	103.3	131.7	172.2[b]			
3-30-7A	28.9	35.0	43.9	51.1	58.9	62.8	65.6	64.4	63.9
3-35-7A	30.6	39.4	50.0	62.2	76.7	87.8	85.0	----	82.2
3-45-7A	26.1	----	31.7	36.7	40.6	43.3	45.0	45.6	45.6
3-40-7A	26.1	30.0	34.4	41.7	47.8	53.3	57.2	----	61.1
3-50-7A	31.1	33.9	37.8	43.3	48.9	53.3	55.6	56.1	56.1
3-60-7A	23.9	26.1	28.9	33.3	37.8	42.2	45.0	46.1	46.7
3-70-7A	22.8	23.9	25.0	28.3	31.7	36.1	38.9	39.4	39.4

Hardness[c]

Ident No.	Before test	After test
2-25-7A	94 A	94 A
2-30-7A	96 A	96 A
2-40-7A	100 A	100 A
2-50-7A	48 D	48 D
3-25-7A	91 A	fail[b]
3-30-7A	95 A	95 A
3-35-7A	96 A	96 A
3-45-7A	98 A	98 A
3-40-7A	96 A	95 A
3-50-7A	95 A	95 A
3-60-7A	98 A	99 A
3-70-7A	50 D	50 D

[a]5 MPa maximum load, 20 Hz, 200,000 cycles, starting temp. 21.1°C
[b]failed at 32,500 cycles
[c]according to ASTM D 2240 Shore A and D

Figure 22. Compressive Fatigue Tests.
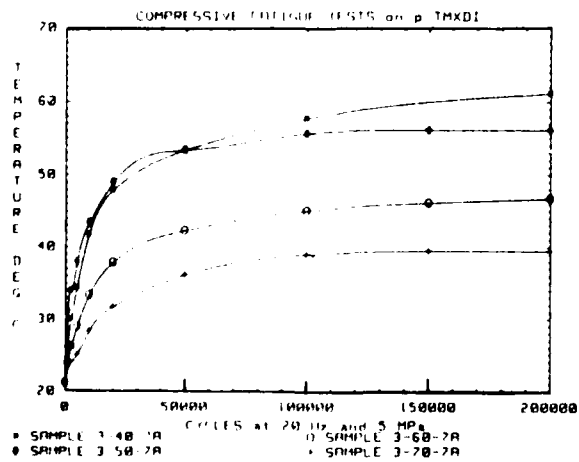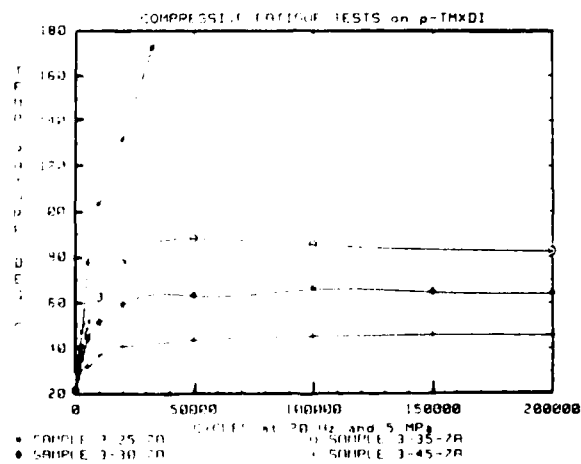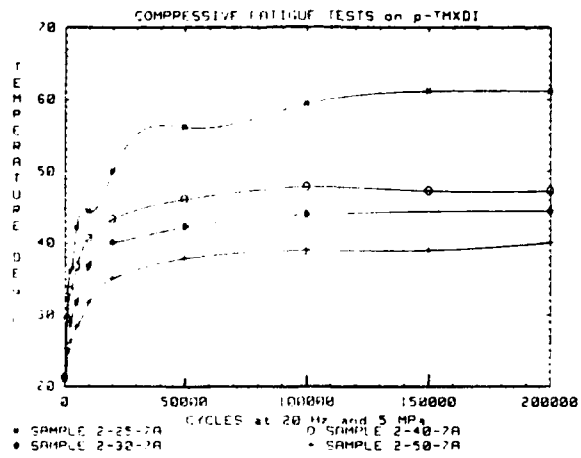
Figure 23. Hardness Test Probes (ASTM D 2240).
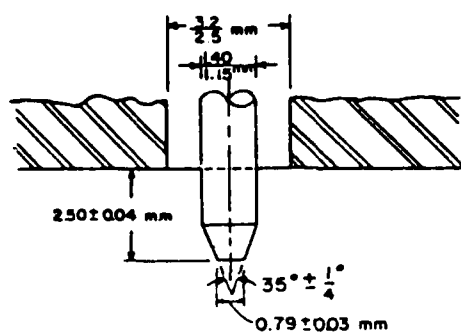
FIG. 1 Indentor for Type A Durometer
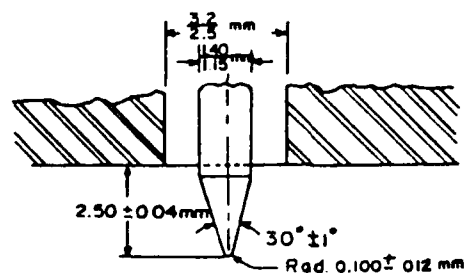
FIG. 2 Indentor for Type D Durometer

Figure 24. FTIR of Me-TMX-Me (Perkin Elmer).

53
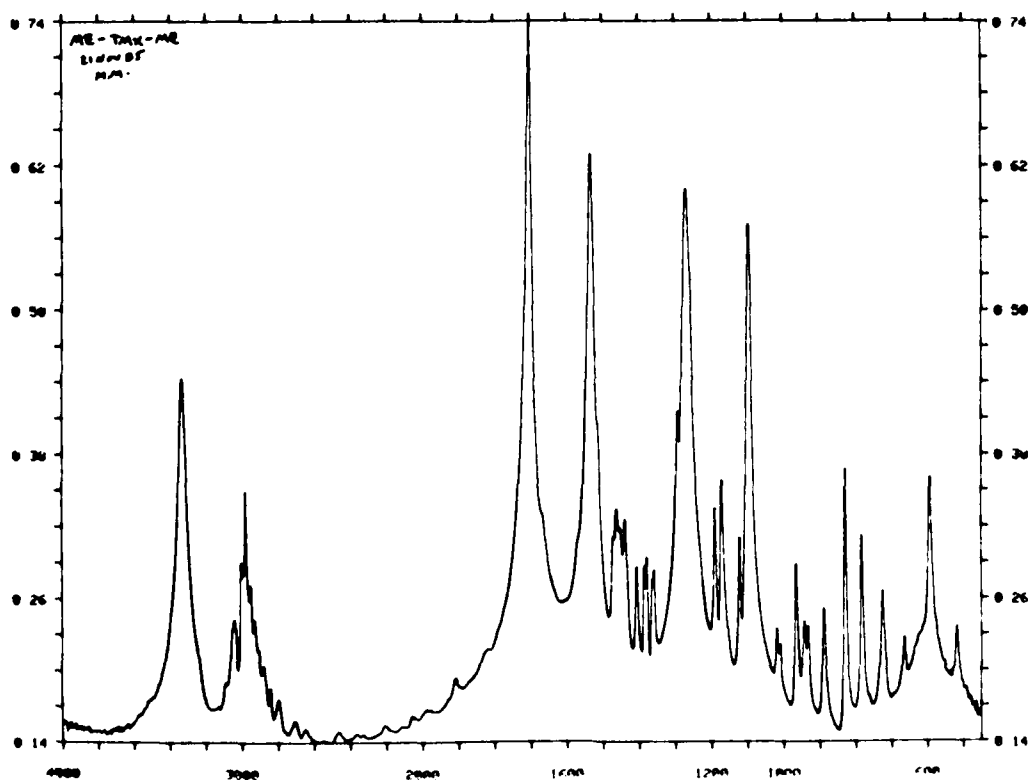
N-H (3330 cm^{-1}) and carbonyl (1700 cm^{-1}) absorbances. Figure 25 shows the mass spectrum, with some of the probable fragments in Figure 26. Figures 27 and 28 show the ^1H and ^{13}C NMR spectra and the resonanace assignments (JEOL 200 MHz NMR). The spectral data for Et-TMX-Et (M.P. 168^oC by DSC) is presented in Figures 29-33. (Spectral assignments were made by consulting Ref. 65.)

X-ray crystallographic data was also collected on these model compounds (analysis by Dr. Jerry P. Jasinski)[66]. Table 9 gives the significant measurements obtained, with Fig. 34 showing the molecular conformation and the numbered atoms. It is noted that these compounds have managed to crystallize in a conformation which permits hydrogen bonding in spite of the steric hindrance caused by nearby methyl groups.

F. WAXS Patterns

Figures 35 and 36 display, respectively, the raw data for an amorphous pattern of a typical HER-extended sample (data collected for only 5 minutes) and a pattern of a crystalline BD-extended sample. The intensity and sharpness of the peaks increased as p-TMXDI equivalents increased in BD-extended samples while soft segment molecular weight was held constant. Higher molecular weight soft segment samples (PTMO 2695) gave slightly sharper peaks than the other samples (PTMO 1934). The approximate percentage of crystallinity in BD-extended samples is presented in Table 10. The approximation was obtained by dividing the sum of the peak areas by the total area (as illustrated in Fig. 37).

Figure 25. Mass Spectrum of Me-TMX-Me.
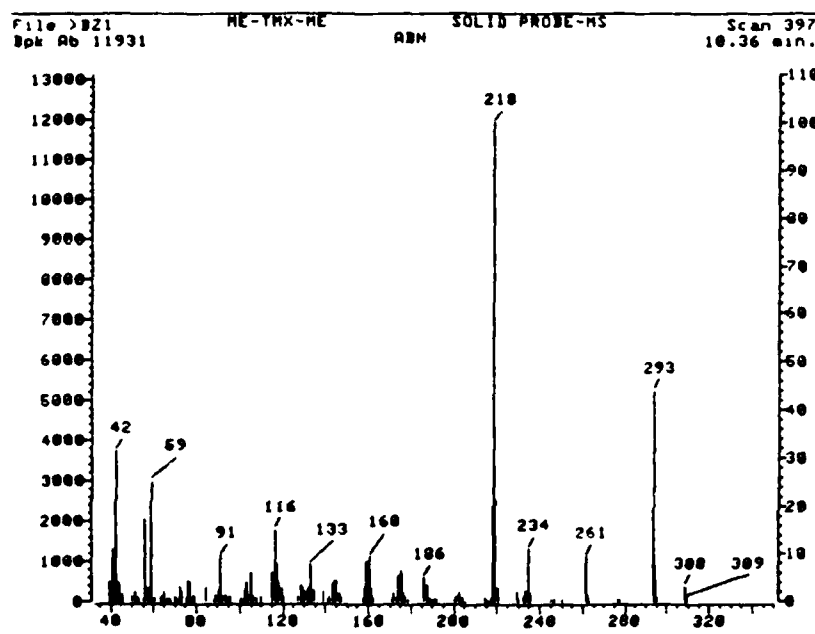
(Hewlett Packard Model 5996 GC/MS System, Al Deome (Operator, PRD))

(Polymer Research Division, Army Materials Technology Laboratory)
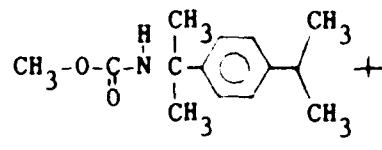
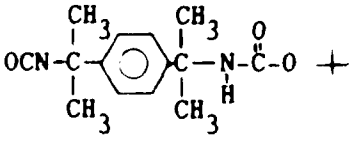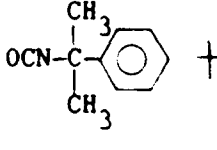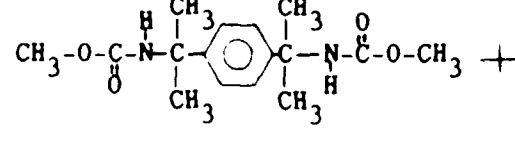Figure 26. Me-TMX-Me Mass Spectrum Fragments.
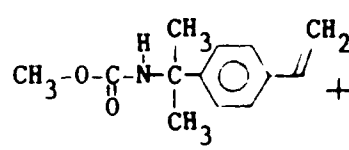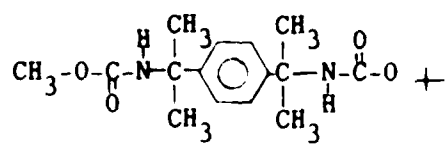
Ion Mass | Ion Detected

218

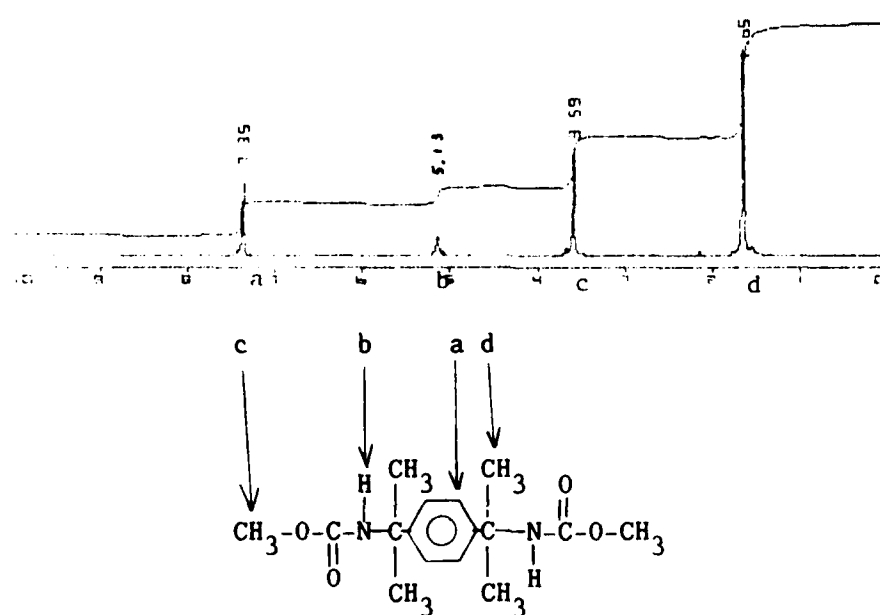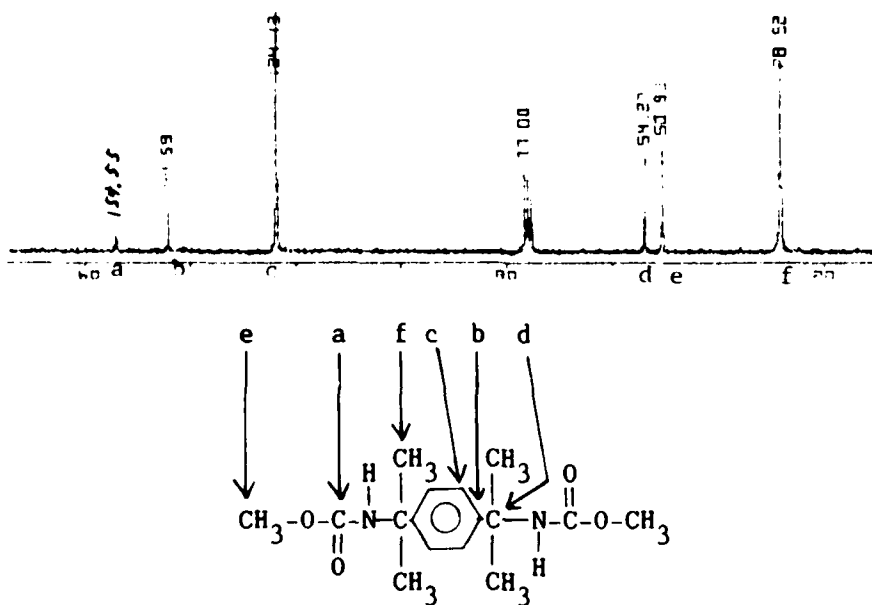293

234

261

160

308

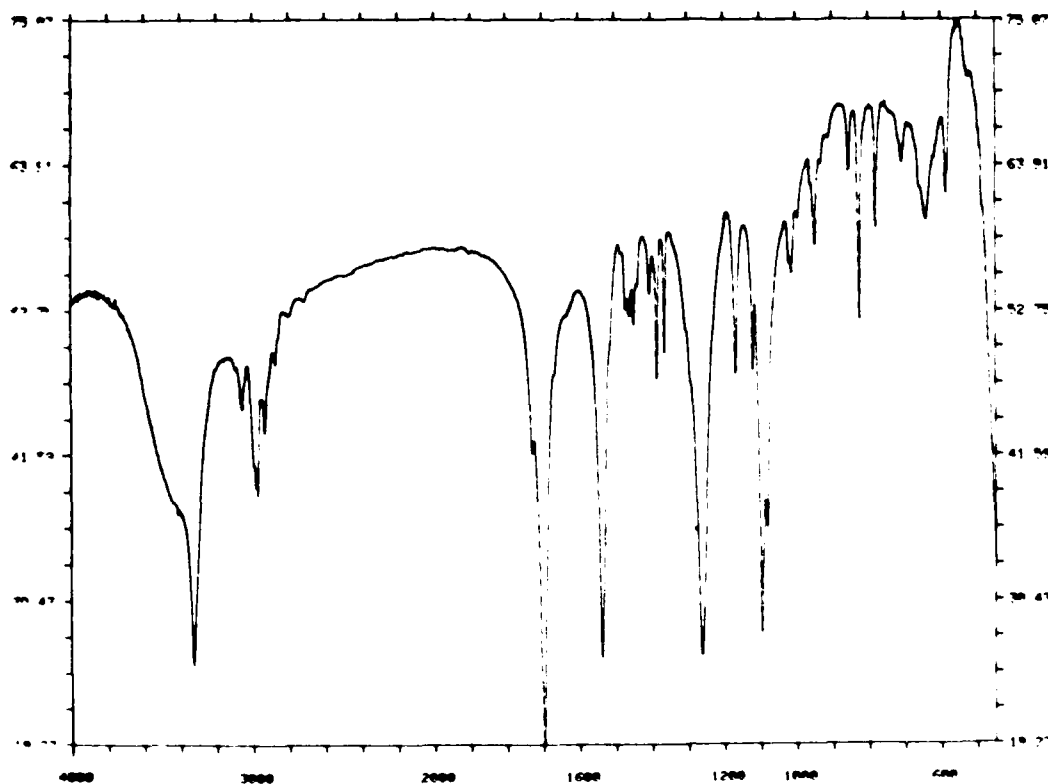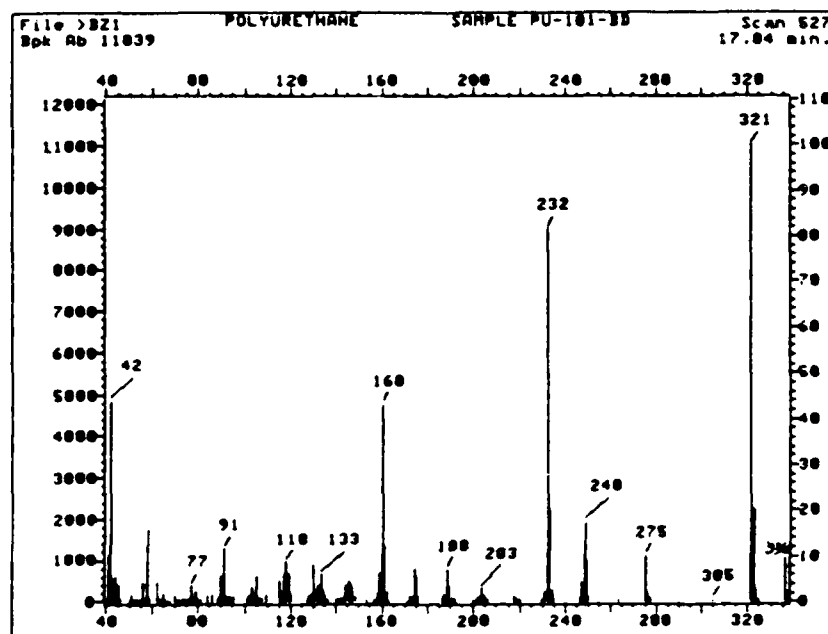Figure 27. ^{1}H NMR of Me-TMX-Me.

Figure 28. ^{13}C NMR of Me-TMX-Me.

Figure 29. FTIR
of Et-TMX-Et.
(Perkin Elmer)

Figure 30. Mass Spectrum of Et-TMX-Et.

(Hewlett Packard Model 5996 GC/MS System, Al Deome (Operator, PRD))

(Polymer Research Division, Army Materials Technology Laboratory)

Figure 31. Et-TMX-Et Mass Spectrum Fragments.

Ion Mass	Ion Detected

321

232

160

275

248

336

Figure 32. ^{1}H NMR of Et-TMX-Et.

Figure 32. ^{1}H NMR of Et-TMX-Et.

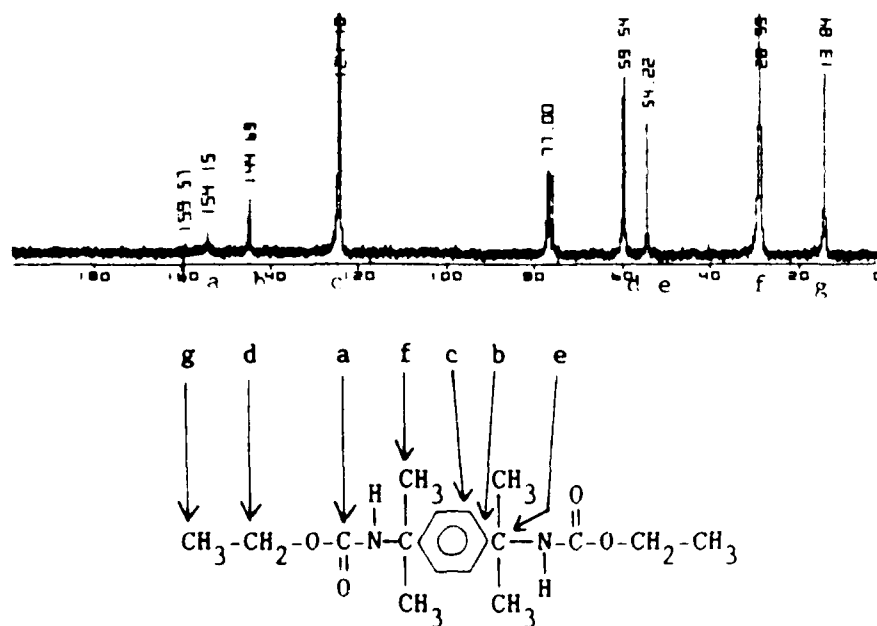Figure 33. ^{13}C NMR of Et-TMX-Et.
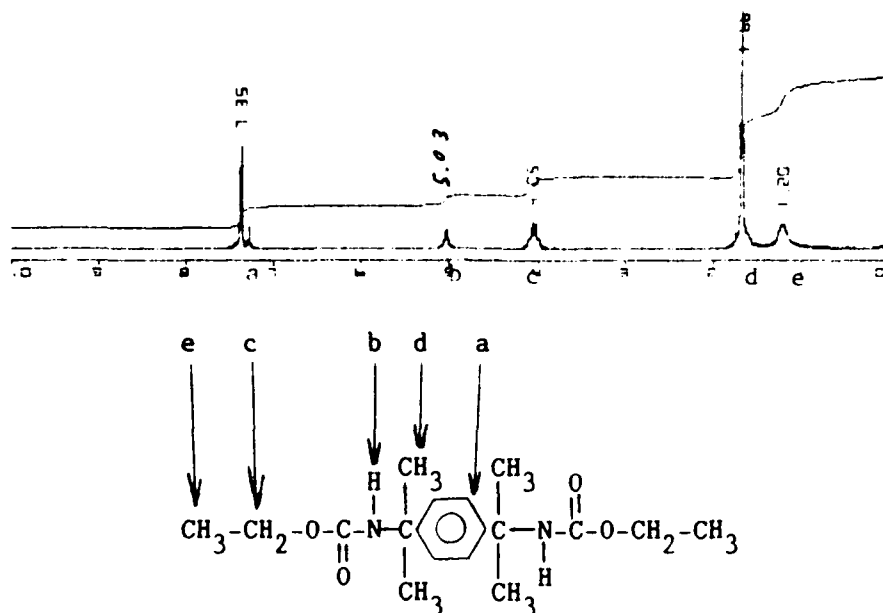
Figure 33. ^{13}C NMR of Et-TMX-Et.

Table 9. Crystallographic Coordinates ($\times 10^4$) for Et-TMX-Et[a] (Ref. 66).

Monoclinic, C 2/c, a=18.653(5), b=11.063(4), c=9.697(3) Å, β=95.39(2)$^{\circ}$, V=1992(1) Å^3, Z=4, d_c=1.129 g cm^{-3}, MoKα (λ=0.71073 Å), u_a(MOKα)=0.07 mm^{-1} at 293 K, R_1=0.056, R_2=0.056, 1363 reflections.

Type[b]	x	y	z
O(1)	2(1)	-670(3)	299(3)
O(2)	2095(2)	-107(4)	-1410(3)
N(1)	3103(1)	646(3)	784(3)
C(1)	3721(2)	1420(4)	536(4)
C(2)	4377(2)	669(4)	222(4)
C(3)	4899(2)	1107(4)	-565(4)
C(4)	5500(2)	451(4)	-784(4)
C(5)	3901(2)	2090(4)	1898(4)
C(6)	3505(3)	2335(5)	-624(6)
C(7)	2753(3)	-49(5)	-229(5)
C(8)	1762(3)	-1429(6)	-625(7)
C(9)	1101(3)	-931(7)	-957(9)
H(N1)[c]	2976(16)	533(31)	1626(36)
H(3)	4824	1892	-978
H(4)	5846	793	-1346
H(5a)	4304	2622	1841
H(5b)	4011	1518	2632
H(5c)	3486	2553	2084
H(6a)	3863	2946	-712
H(6b)	3068	2707	-388
H(6c)	3415	1910	-1486
H(8a)	1702	-2194	-183
H(8b)	1990	-1551	-1461
H(9a)	842	-430	-366
H(9b)	765	-1395	-1554
H(9c)	1383	-432	-1508

[a] The numbers in parentheses are the estimated standard deviations in the last significant digit.

[b] Atoms are labeled in agreement with Figure 34.

[c] All the hydrogen atoms which are covalently bonded to carbon atoms carry the same numerical subscript as the carbon atom to which they are bonded with the additional literal subscript (a,b,or c) to distinguish between hydrogen atoms bonded to the same carbon except for the hydrogen atom which is covalently bonded to N(1). This one is labeled H(N1).

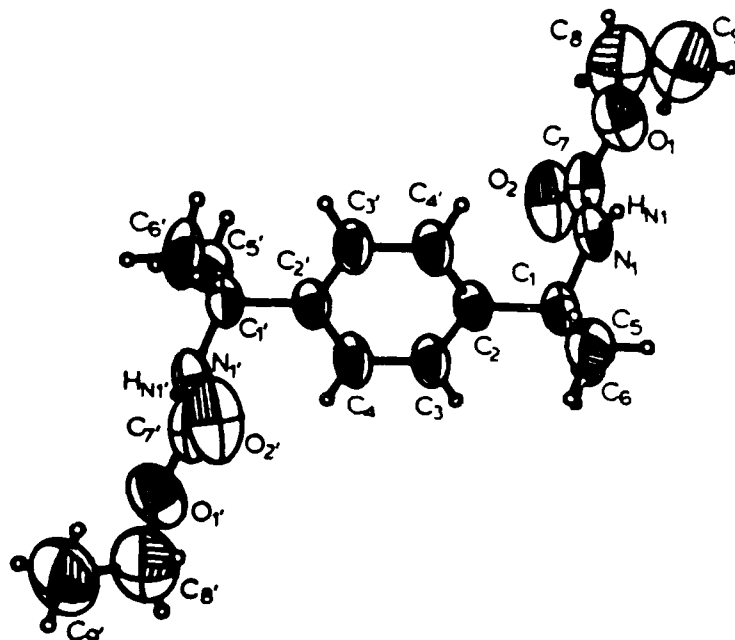Figure 34. Model of Et-TMX-Et (Ref. 66).
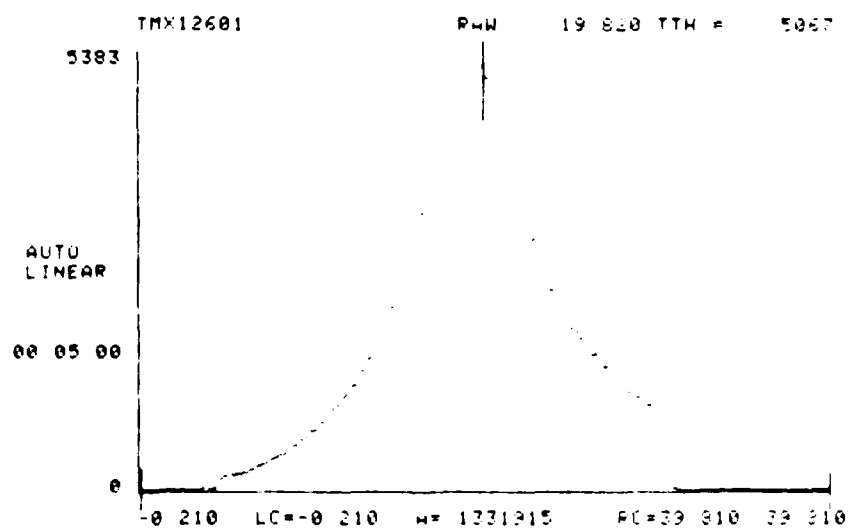

Figure 35. WAXS Pattern of 3-50-25P-R.
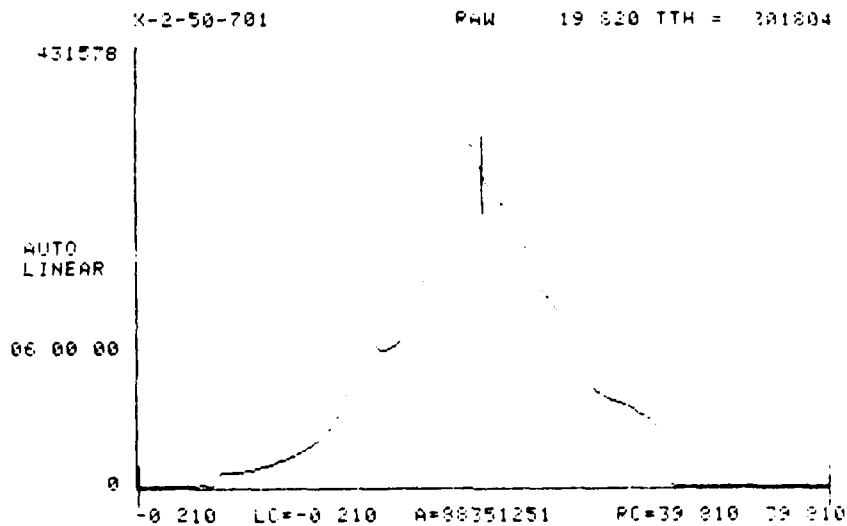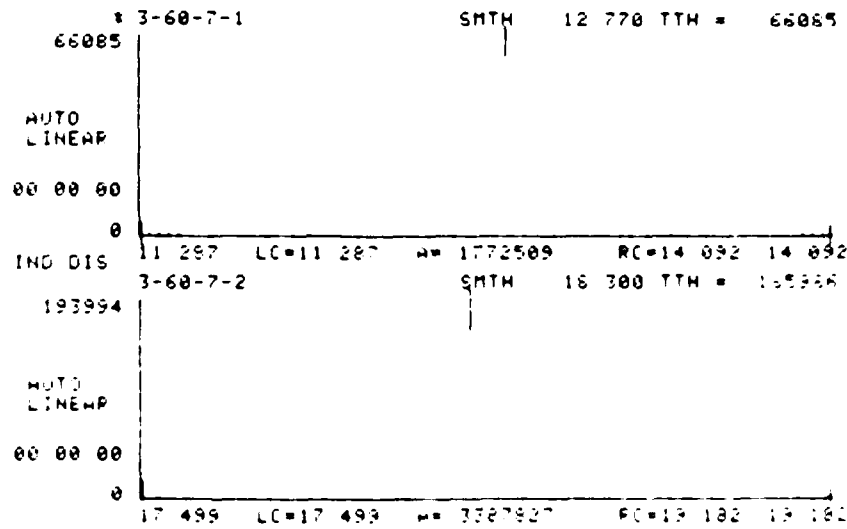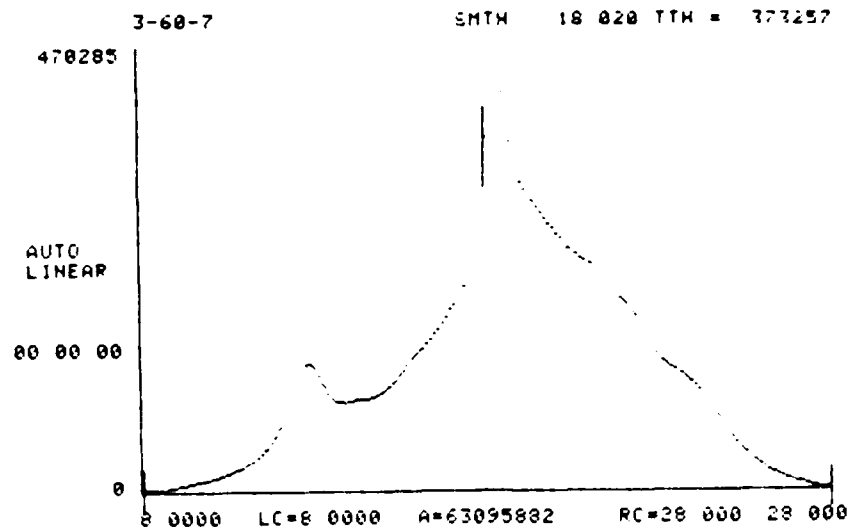
Figure 36. WAXS Pattern of 2-50-7A.

Table 10. Approximate Crystallinity of Selected Samples by WAXS.

Ident. No.	Percent Crystallinity
2-25-7A	4.1
2-30-7A	5.4
2-40-7A	6.4
2-50-7A	7.0
3-40-7A	5.5
3-60-7A	8.2
3-70-7A	9.4

Figure 37. Area Measurements of 3-60-7A.

$$(1772509 + 3387827)/63095882 = 0.082 \ (8.2\%)$$

VI. DISCUSSION

The original idea for this research was based upon the behavior of some elastomer samples of unknown composition which were subjected to cyclic compression testing and showed lower hysteretic heatup than any previously tested elastomer[67]. Figure 38 has the hysteretic heatup curves of three such polyurethanes conjectured to be polyester-based (6, 8A, and 8B) and the curves of three possibly polyether-based samples (3, 4, and IV) with essentially stabilized temperatures after 60,000 cycles (46, 35, and 45°C respectively). It was found, by chemical and other methods, that the latter three unknowns were composed of CHDI, PTMO, BD, and some percentage of TMP (as crosslinker). The molecular weight of PTMO and the ratios of the ingredients remained unknown, but synthesis and testing[61] with known quantities of ingredients in CHDI-based samples allowed the qualitative reproduction of samples similar to the unknowns in their test results. These known samples displayed behavior similar to that of the unknowns, including their hysteresis behavior.

The research reported here explored the properties of polyurethanes based on p-TMXDI. p-TMXDI can be compared to CHDI in several ways:

1. Both produce aliphatic urethanes, although p-TMXDI contains an aromatic ring. Urethanes in which alkoxy-O and amido-N are both covalently bonded to alkyl, rather than aryl, have been found to be the most thermally stable[68] (Table 11).

2. Polyurethanes derived from both, formed with aliphatic urethanes, should be resistant to photochemical decomposition.

65

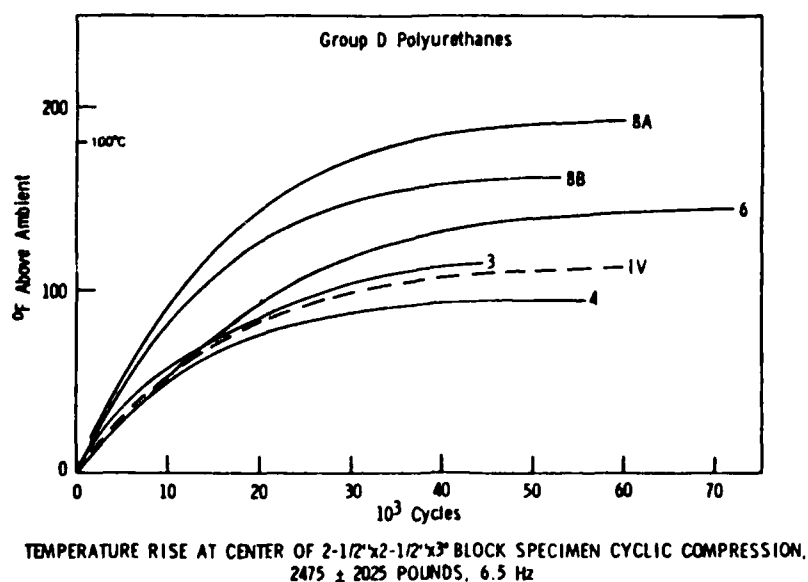Figure 38. Hysteretic Heatup of Polyurethane Unknowns (Ref. 67).

TEMPERATURE RISE AT CENTER OF 2-1/2"x2-1/2"x3" BLOCK SPECIMEN CYCLIC COMPRESSION, 2475 ± 2025 POUNDS, 6.5 Hz

Table 11. Decomposition Temperatures of Urethane Bonds (Ref. 68).

Type of urethane group	Approximate upper stability (^{o}C)
Alkyl-NH-CO-O-alkyl	250
Aryl-NH-CO-O-alkyl	200
Alkyl-NH-CO-O-aryl	180
Aryl-NH-CO-O-aryl	120

66

3.   Polyurethanes derived from both have symmetrical backbones (as do those derived from MDI).   This enhances the probability of formation of crystalline regions within hard segments which have collected before solidification.   Model compounds incorporating either p-TMXDI or CHDI provide evidence of this probable crystalline behavior.

4.   The polymers derived from these diisocyanates have, so far, provided several samples which have good mechanical properties, high resistance to thermal breakdown ($>150^{\circ}$C before softening), and better resistance to hysteretic heatup than other polyurethanes.

In order to understand the behavior of the p-TMXDI-based polyure-thanes, all aspects of the available structural information need to be examined.   Comparisons need to be made, not only with CHDI-based polyu-rethanes, but with other types now in common use. From the evidence of hysteresis behavior in the CHDI- and p-TMXDI-based urethanes, some basic differences must exist between their molecular structures and the struc-tures of other polyurethanes.

Early in this research, a decision was made to examine the effects of different chain extenders on the thermal properties of p-TMXDI-based polyurethanes.   BD was selected for its ability to produce the consist-ently highest softening temperatures[47] of polyurethanes derived from the available straight-chain diols, due to the packing efficiency of the hard-segment chains which BD made with the diisocyanate (usually MDI). HQEE provides good mechanical properties at elevated temperatures in some polyurethanes, but limitations on the preparation temperature and method required substitution of HER.   HEB, which is a derivative of

67

Bisphenol A (HEB minus the hydroxyethyl moieties), has also been tested[55] in some other polyurethanes and found to provide some desirable properties. These chain extenders were expected to promote formation of crystalline hard segment regions, and thus result in polyurethanes resistant to typical thermal and mechanical stresses.

A close examination of model compounds derived from various straight-chain diols is instructive. Those with an even number of carbons in the $(-O-(CH_2)_x-C-)$ moiety, where $x \geq 4$, were found to crystallize in extended conformations in model compounds[47]. (Fig. 2 has x=4 (BD) in the compounds which were studied by Born et al.[47]) The carbonyls at either end of this backbone are oriented in nearly opposite directions in these models, thus resulting in planar urethane (and hydrogen) bonds which face in opposite directions at either end of the chain. Model compounds where x was an odd number of 5 or greater crystallized with planar diol backbones and carbonyls pointed in the same direction. To facilitate hydrogen bonding between chains, the diol backbone is curved sufficiently to reduce the strain which would be present in a completely straight chain (which is formed by the even diols). This still results in longer hydrogen bond distances, and thus higher energy conformations and crystals somewhat less stable than those with even diols. The structures where x=2 or 3 were both crystallized in contracted conformations which had carbonyl alignments similar to their respective even and odd counterparts of greater length.

X-ray diffraction experiments were also run on stretched fibers of MDI-based polyurethanes with various chain extender lengths[43-45]. The data for the even-length chains was in general agreement with the model

compound results, but the odd-length chain data suggested some twisting in the diol chain which would allow the carbonyls at either end to reorient themselves in opposite directions, as in the even length chains. The polyurethane with the diol x=2 (ethylene glycol) was postulated to have carbonyls oriented at ~90° to each other at either end of the diol chain.

These differences between the models and the stretched fibers for x=2 and x=odd are due to limitations imposed on the longer hard-segment fibers which possess more than two urethane moieties in each polar section of the chain, and are required to hydrogen bond as many sites as possible to achieve the lowest possible energy state of the crystal form. For example, in hard segments incorporating even diol chains, such as butanediol residues, the MDI phenyl rings are free to rotate about the $-CH_2-$ center. The two carbonyls which are connected by an even diol unit in a hard segment chain are oriented at 180° to each other, as in the model compound (MMI-BD-MMI), but are oriented at 90° to the carbonyls in an adjacent diol section. In this conformation, the layers of chains which would form in a crystalline hard segment region are hydrogen bonded "in the viewing plane" in one diol section and "perpendicular to the viewing plane" in adjacent diol sections connected by the diphenylmethane moieties (Fig. 39). The hard segments with odd chain diols are also configured to minimize energy. Since crystal packing of larger molecules inhibits the curved backbone seen in the

Figure 39. Models of MDI Hard Segments from Blackwell and Born[48].
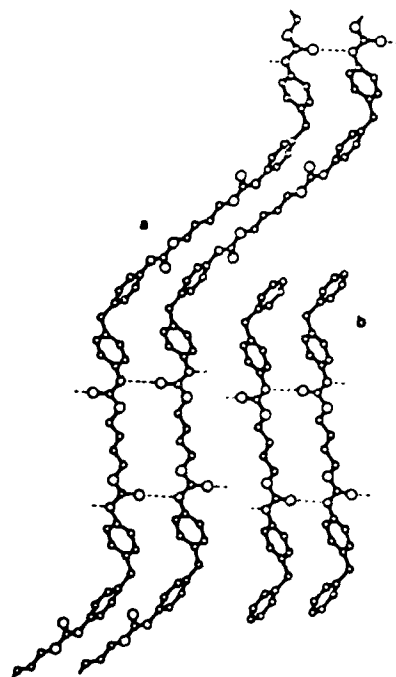
models, the chain sections are twisted into suitable conformations compatible with this requirement. Proposed conformations of polyurethanes incorporating odd diol moieties suggest only a two dimensional hydrogen bonding network (i.e. all hydrogen bonding "in the viewing plane"). In the case of x=2, the carbonyls at either end of each ethylene dioxy chain are thought to be oriented at ~90° to each other, allowing a three dimensional hydrogen bonding network.

These chain conformations of the various diol-MDI polyurethanes affect the thermal properties of the polymers. The melting points of the model compounds with x=even are all at least 10°C higher than when x=odd[47]. This is a direct result of the hard-segment conformations, with the hard segments derived from even-numbered diol units assuming more tightly packed structures, leading to shorter hydrogen bonds and higher melting points. In higher molecular weight chains (e.g. hard segments in polyurethanes) the polymers with x=4 (i.e. BD) usually have the highest softening temperatures, a probable result of the three dimensional hydrogen bond network and the short chain-extender which keeps adjacent hydrogen bonds closer than longer chain-extenders.

The formation of crystalline model compounds of both p-TMXDI and CHDI is highly suggestive of crystallite formation in their respective polyurethanes. Most CHDI-based polyurethanes, which have been prepared and tested in known formulations[61], developed high-temperature resistant regions in the polymer matrix, usually softening (TMA) above 225°C. (These experiments used primarily BD as chain extender.) The BD-extended samples of p-TMXDI-based polymers usually softened above 175°C. These

71

relatively high softening temperatures for both types of polymers are also indications of crystalline content. With low crosslinker content in the samples, crystallization driven by hydrogen bonding is the most likely reason for their thermal stability.

The use of HER and HEB as chain extenders for p-TMXDI is apparently of little value when thermal stability is a primary concern. The TMA data is definitive evidence of some fundamental structural difference concerning the chain extenders. The DSC results for the apparent heats of fusion (joules/gram) show another difference between chain extenders. Those samples containing HER or HEB have total melting transitions of less than 5 joules/gram (including the crosslinked HER samples), while most samples with BD require at least 10 joules/gram for their transitions. This is a further indication of more crystalline content in p-TMXDI polymers utilizing BD as the chain extender.

The infrared spectra of p-TMXDI-based polymer samples is another indication of major differences between chain extenders. The IR spectra of all BD-extended samples are almost identical to Figure 20 in appearance, with a strong N-H absorption (hydrogen bonded) and a carbonyl absorption (hydrogen bonded) with small free carbonyl shoulder. A strong resemblance is noted in these regions between the spectra of polymer samples and of the model compounds (Figs. 24, 29). The N-H and carbonyl signals are indications of a high percentage of hydrogen bonding in the polyurethane samples. Figure 21 is representative of the FTIR spectra of HER- and HEB-extended samples, with weaker and broader N-H absorptions, and carbonyl hydrogen-bonded and free absorptions of roughly equal intensity. This is an indication of a much lower percent-

72

age of hydrogen bonding in these samples, a condition which was reflected in the thermal behavior of these samples.

The introduction of HER or HEB as chain extenders with p-TMXDI introduces some obvious disruptions into the hard-segment region, an environment where crystallinity is the preferred state and is partly driven by hydrogen bonding. An assumption concerning the chain extender behavior is that BD fits the necessary crystalline conformation as part of the chain, while HER and HEB, although they may produce crystalline solids, assume a conformation different from the crystalline structure of a p-TMXDI urethane moiety (possibly an incompatible crystalline space group). HER and HEB have been used with MDI and produced polyurethanes with good properties. A conformational resemblance can be noted between the MDI and HEB molecules, a symmetry which probably enhances their compatibility. HER, although it is not symmetrical, has the flexibility and absence of steric hindrance with MDI to fit into a crystalline stacking arrangement with one of the MDI urethane rings.

The hard segments of MDI-based polyurethanes possess some degree of flexibility with regard to chain extenders. As mentioned previously, different carbonyl conformations were possible depending upon the number of carbons in the straight chain diols. A three dimensional network of hydrogen bonds is possible due to the freedom of movement about the central $-CH_2-$ in MDI urethanes. This flexibility can be expected with polyurethanes derived from compatible aliphatic diols and aromatic diols

73

(e.g. HQEE, HER, HEB).

p-TMXDI has more stringent requirements with regard to conformation. The model compounds derived from p-TMXDI show the steric effect of methyl groups adjacent to both the aromatic ring and the urethane bond. Although the model derived from MDI, by end-capping with methoxy, crystallized into one of two possible conformations, p-TMXDI crystallized in a conformation which is expected to be its only possible conformation. The p-TMXDI molecule has no central point of rotation (which the $-CH_2-$ moiety gives to MDI), a limitation expected to inhibit the three dimensional hydrogen bonding effect which is proposed for MDI-based polyurethanes. CHDI-based polyurethanes are expected to display a restriction similar to p-TMXDI derivatives, probably with the CHDI-urethane moieties assuming a stacked chair conformation and the carbonyls approximately perpendicular to the plane of the ring (similar to the p-TMXDI-based models). Three dimensional hydrogen bonding networks for p-TMXDI-based urethanes would originate from a change in conformation of the chain extenders.

The actual structural arrangement of p-TMXDI hard-segment regions probably involves different degrees of crystallinity, and possibly different conformations (which are influenced by factors which were mentioned in Chapter II, the literature review). First, variations between samples are dependent on the molecular weight of the PTMO soft-segment. More opportunity for phase separation is provided by higher-molecular-weight polyethers. Second, the number of equivalents of p-TMXDI in any sample will determine the average hard-segment chain length and the average size of the hard-segment region in the chain

direction. Third, the type and length of the chain extender determines the final conformation. Fourth, the presence of crosslinker will reinforce the hard segment region, but at the same time it will locally disrupt any crystalline regularity. Other factors will also play a role in the different arrangements of chains.

The thermal transition information collected by DSC is an indication of the complexity present in the different polyurethane samples. Two (and sometimes three) melting transitions were noted for the sheet samples. In the block samples, a more uniform behavior is presented by the two melting transitions of each sample. However, differences exist between samples concerning the first melting transition temperature and the ratio of the heats of fusion of the two transitions in each sample. Some DSC results even showed an exothermic transition between the melting transitions, indicating that crystallization was initiated by the freedom of movement at that temperature. These observations lead to the conclusion that two different types of hard segment regions exist in the block samples.

The thermal behavior of the p-TMXDI hard-segments extended by BD may be attributed to some possible variations in different hard-segment regions. Different regions may contain different numbers of equivalents of p-TMXDI (e.g. one sample may have regions with four equivalents and others with five). The chain extender may be arranged in different conformations: the work of Blackwell[43-45] and Briber and Thomas[53] suggests that BD can assume both a contracted and an expanded confor

mation, leading to two different packing efficiencies (with the extended conformation most likely possessing a higher melting temperature). The p-TMXDI moieties are probably not stacked uniformly and may resemble the packing arrangement which was suggested by Bonart[33] (Fig. 40), where layers of MDI moieties alternate with layers of BD residues. The thermal differences may also be due to the efficiency with which the different regions have crystallized (i.e. crystalline or moderately amorphous); this is unlikely, since a variation in crystallinity would be expected to produce transitions at several different temperatures for several possible degrees of crystallinity. Determining the most probable explanation will require further preparation and analysis of model compounds and polyurethanes.

The WAXS patterns of the p-TMXDI/BD/PTMO polyurethanes are further indications of crystallinity. Figure 36 shows a pattern with sharp reflections at angles (2θ) of ~18.3° and ~12.7°. These correspond, by the formula $n\lambda = 2d \sin\theta$, to measurements of ~4.8Å and ~6.9Å respectively. In MDI-based polyurethanes, the WAXS reflections were assigned to different spacings of the hard segment chains. The model compound unit cells were also distorted from monoclinic to triclinic unit cells to simulate the molecular arrangement of the chains. A similar process is planned for the p TMXDI models; this should allow relation of crystalline reflections to characteristics of the hard segment crystalline regions.

The compressive fatigue testing of the block samples demonstrates

Figure 40. MDI Stacking Arrangement Proposed by Bonart (Ref. 33).
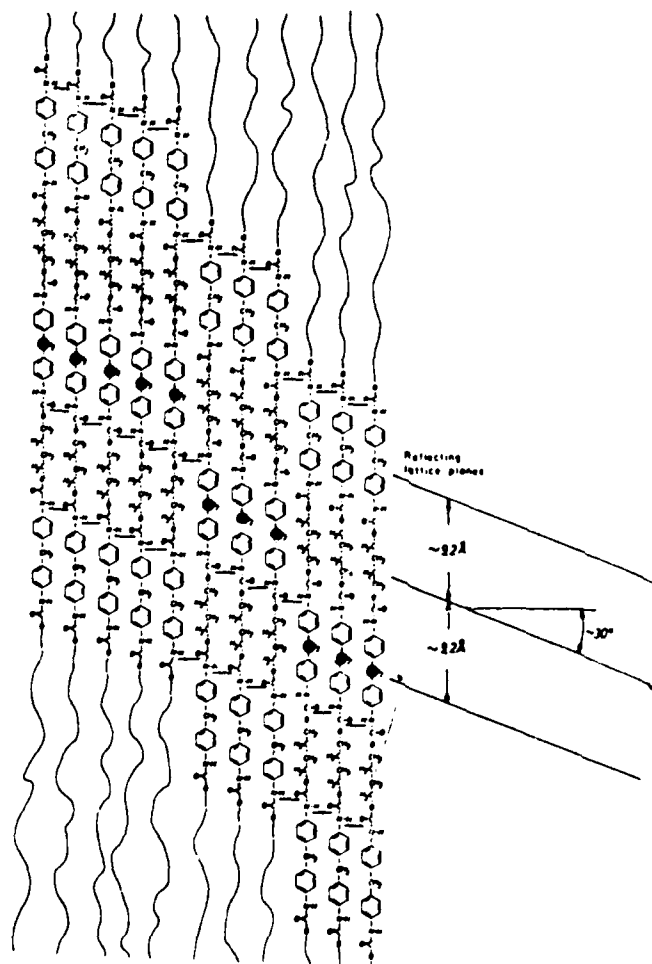
their resistance to excessive hysteretic heatup. Progressively higher hard-segment content in the samples produced progressively less hysteretic heat. Sample 3-25-7A was the only sample to fail. The other samples remained below $100^{o}C$ and may be expected to retain most of their mechanical strength at these operating temperatures (Fig. 22).

The polyurethanes made with CHDI and with p-TMXDI have two important characteristics in common which set them apart from most other polyurethanes: 1. They are both resistant to compressive fatigue heatup. 2. They are both expected to crystallize exclusively into two dimensional bonded networks (one direction represented by the covalently bonded chains, the other by hydrogen bonding) (Intermolecular van der Waals forces provide integrity in the third direction.) MDI based polyurethanes have already been shown to assume three dimensional and other varied combinations. 2,4- and 2,6-TDI do not possess the higher symmetry of the other three diisocyanates. H_{12}MDI is normally a mixture of isomers; even the trans-trans isomer might have some difficulty crystallizing into a compact conformation. Other diisocyanates have either other restrictions on good crystallization or excess flexibility in their structure (e.g. hexamethylene diisocyanate).

The reason for the resistance to hysteretic heat buildup of CHDI and p-TMXDI based polyurethanes is an unknown to be explored in future research. Two possible explanations are: 1. The highly crystalline regions expected in the polyurethanes are especially rigid and resistant to mechanical deformation which would release heat upon relaxation. 2. The crystalline regions are oriented and transmit thermal energy along some axis to the surface regions. This second possibility is somewhat

78

speculative, but similar behavior has been seen in other materials. The two explanations are not mutually exclusive.

The p-TMXDI-based materials have exhibited one undesirable characteristic. Crystals of freshly-prepared model compound which were dissolved in tetrahydrofuran (THF) to test for purity by chromatography (HPLC), upon analysis by HPLC after one day in solution, showed accumulation of another component with slow loss of the model compound. GC/MS analysis indicated formation of an isopropenyl moiety in place of the urethane bond at one end of the model compound (Fig. 41). A speculation was made that traces of acid (the glassware had been washed with chromic acid, then rinsed several times) and peroxide caused the decomposition of the model compound. p-TMXDI is manufactured, according to the patent[62] (Fig. 42), using an acidic step to form a urethane. Reversal of the reaction is possible under the proper conditions.

Later attempts were made to repeat the decomposition reaction under controlled conditions. Crystals run at a later date, in THF solution in glassware washed with acid, showed no signs of decomposition. A solution of freshly prepared crystals in THF with traces of methanol was found to be stable. Also, crystals which had been exposed to the humid air for a few weeks were also stable in the THF solution. The presence of hydroxyls may serve to protect the urethane by some mechanism. Therefore, polyurethanes containing p-TMXDI as the prime constituent are not expected to be susceptible to decomposition from exposure to typical environments, such as the weather. However, they may be sensitive to acids or peroxides under arid conditions. This is a matter for further investigation.

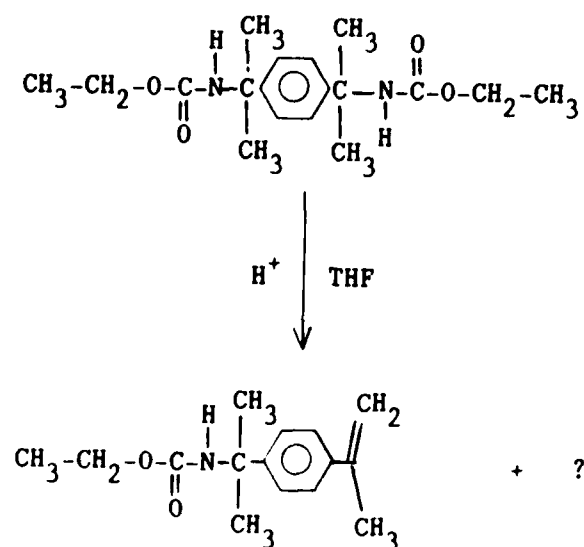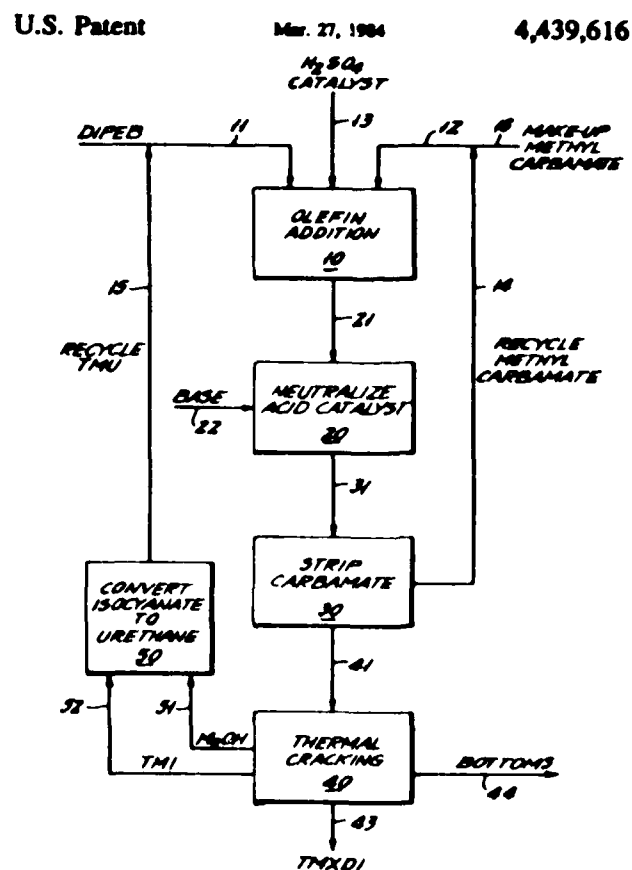79

Figure 41. Possible Decomposition of Et-TMX-Et.

$$CH_3-CH_2-O-\underset{\underset{O}{\|}}{C}-\underset{\underset{H}{|}}{N}-\underset{\underset{CH_3}{|}}{\overset{\overset{CH_3}{|}}{C}}\langle\bigcirc\rangle\underset{\underset{H}{|}}{\overset{\overset{CH_3}{|}}{C}}-\underset{\underset{CH_3}{|}}{N}-\underset{\underset{O}{\|}}{\overset{\overset{O}{\|}}{C}}-O-CH_2-CH_3$$

$$H^+ \Big| \ THF$$

$$CH_3-CH_2-O-\underset{\underset{O}{\|}}{C}-\underset{\underset{H}{|}}{N}-\underset{\underset{CH_3}{|}}{\overset{\overset{CH_3}{|}}{C}}\langle\bigcirc\rangle\underset{\underset{CH_3}{|}}{\overset{\overset{CH_2}{\|}}{C}} \quad + \quad ?$$

Figure 42. Patent Preparation of p-TMXDI (Ref. 62).

80

VII. CONCLUSIONS

p-TMXDI has been mixed with different chain extenders and various molecular weight soft segments and percentages of crosslinkers. The resulting polyurethane samples have been subjected to thermal, mechanical, and spectral tests to determine the structural content of each preparation and the behavior of each sample under various stresses. Model urethane compounds were also prepared from p-TMXDI to simulate the ideal hard-segment crystallization and determine the possible structural arrangement of the hard segments in the polyurethane samples.

When resistance to high temperatures (up to 150°C) is necessary, a chain extender composed of a straight chain aliphatic diol is required for p-TMXDI-based polyurethanes. Butanediol, which is commonly used for other urethanes, allows sufficient separation between methyl units in adjacent p-TMXDI moieties to avoid steric hindrance during and after reaction. It also minimizes the distance between hydrogen bonds, resulting in a higher density of hydrogen bonds and leading to higher softening temperatures for the p-TMXDI-based polyurethanes.

The presence of crystalline regions in p-TMXDI-based polyurethanes is indicated by different analyses. Differential scanning calorimetry data indicates high temperature (>150°C) melting transitions, usually two, are present in all polymer samples containing butanediol as the chain extender. Wide angle X-ray scattering data shows two reflections which both grow in relative intensity as the percentage of hard segment material is increased in the various preparations. The uncomplicated preparation of crystalline model compounds is another indication that

81

crystallinity in the hard segment regions is highly probable.

Compressive fatigue testing results demonstrate the resistance of some p-TMXDI-based polyurethanes to hysteretic heatup. Although only blocks with high hard-segment content, and high hardness values, have been tested, blocks with lower hard-segment content are expected to reach steady-state temperatures during compressive fatigue tests. Steady-state temperatures which are well below the softening temperatures of the polyurethanes (e.g. $<100^{\circ}C$) are preferred to allow retention of good mechanical properties. A compromise in the hard segment content would be necessary to balance the desirability of a softer polyurethane against the need to avoid high internal tempera tures.

VIII. SUGGESTIONS FOR FURTHER RESEARCH

1.   Additional block samples with different NCO/OH ratios are needed to examine the effects of variations in the diisocyanate/hydroxyl ratio during hysteresis testing.   In other research[61], variations in NCO/OH ratios have produced some significant changes in properties.   (The samples in this research were all 1.05:1.00.)

2.   Solid samples can now be examined using FTNMR with solid state probes.   Scanning the polyurethanes in solution or after pulverization does not provide the potentially valuable information about chain packing, conformation, and hydrogen bonding which is anticipated from the solid phase NMR equipment which has recently become available.   Relatively little research has been published concerning NMR of solid polyurethanes.

3.   A model compound analogous to MMI-BD-MMI may be prepared from p-TMXDI (Fig.   43).   This would be useful in X-ray crystallography for determining the chain extender conformation.

4.   A diacetylene chain extender (Fig. 44) may be used to raise the softening temperature and improve the high temperature resistance and integrity of polyurethane hard-segments[69]. The diacetylene moieties may be polymerized, after the polyurethane has been cured, by heat or γ radiation.   This would result in a polydiacetylene network which would reinforce the structure of the hard segment by creating extensive crosslinks.

Figure 43. Model Preparation of TMX-BD-TMX.
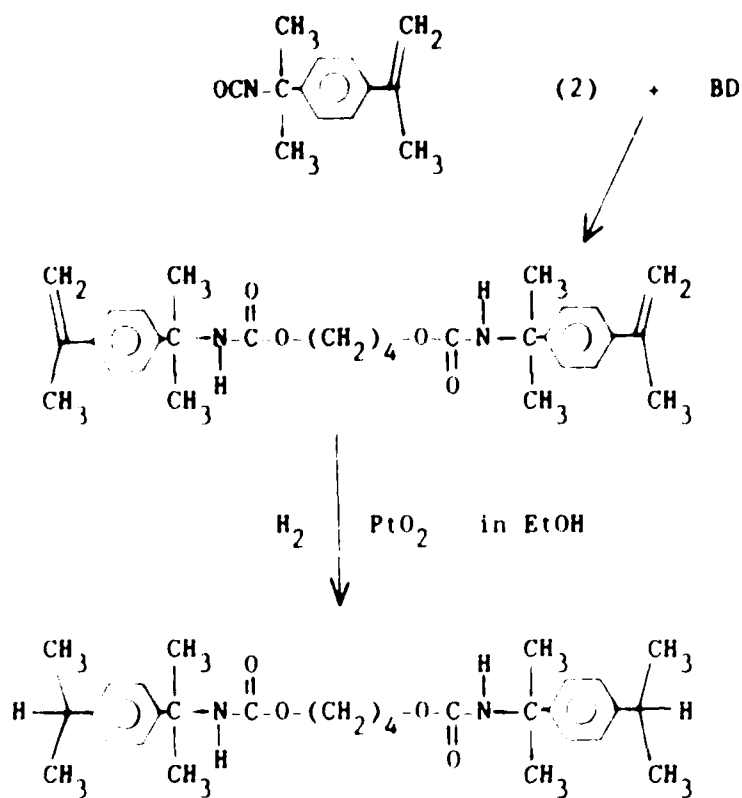
Figure 44. Diacetylene Diol Crosslinker as Chain Extender (Ref. 69).
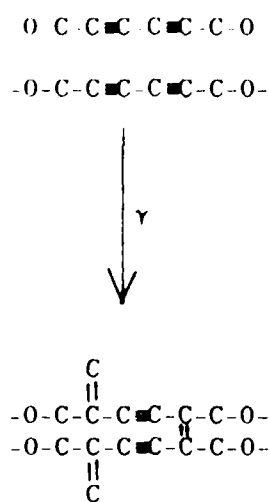
IX. GLOSSARY

BD   butanediol

CHDI   cyclohexyldiisocyanate

DBTDL   dibutyltin dilaurate

DSC   differential scanning calorimetry

EG   ethylene glycol

GC/MS   gas chromatography/mass spectroscopy

HD   hexanediol

HEB   hydroxyethyl bisphenol-A

HER   hydroxyethyl resorcinol

$H_{12}MDI$ methylene-bis(cyclohexylisocyanate)

HQEE   hydroxyquinone ethyl ether

HTPBD   hydroxy-terminated polybutadiene

MDI   methylene-bis(phenylisocyanate)

MMI   4-benzyl phenyl isocyanate

PTMO   poly(tetramethylene oxide)

SAXS   small angle X-ray scattering

T_c temperature of crystallization

TDI   toluene diisocyanate

TEA   triethanolamine

T_g glass transition temperature

TGA   thermogravimetric analysis

T_m melting transition temperature

TMA   thermomechanical analysis

TMP   trimethylolpropane

TMXDI   tetramethylxylene diisocyanate

WAXS   wide angle X-ray scattering

X. REFERENCES

1. Cooper,S.L.,Tobolsky,A.V.;J.Appl.Poly.Sci. 10 1837 (1966).

2. Schneider,N.S.,Sung,C.S.P.;Poly.Eng.Sci. 17 (2) 73 (1977).

3. Xu,M.,MacKnight,W.J.,Chen,C.H.Y.,Thomas,E.L.;Polymer 24 1327 (1983).

4. Chen,C.H.Y.,Briber,R.M.,Thomas,E.L.,Xu,M.,MacKnight,W.J.;Polymer 24 1333 (1983).

5. Camberlin,Y.,Pascault,J.P.;J.Poly.Sci.Poly.Chem. 21 415 (1983).

6. Camberlin,Y.,Pascault,J.P.;J.Poly.Sci.Poly.Phys. 22 1835 (1984).

7. Hwang,K.K.S.,Lin,S.B.,Tsay,S.Y.,Cooper,S.L.;Polymer 25 947 (1984).

8. Miller,J.A.,Lin,S.B.,Hwang,K.K.S.,Wu,K.S.,Gibson,P.E.,Cooper,S.L.; Macromolecules 18 (1) 32 (1985).

9. Abouzahr,S.,Wilkes,G.L.;J.Appl.Poly.Sci. 29 2695 (1984).

10. van Bogart,J.W.C.,Gibson,P.E.,Cooper,S.L.;J.Poly.Sci.Poly.Phys. 21 65 (1983).

11. Miller,J.A.,Cooper,S.L.;J.Poly.Sci.Poly.Phys. 23 1065 (1985).

12. West,J.C.,Cooper,S.L.;J.Poly.Sci.Poly.Symp. 60 127 (1977).

13. Sung,C.S.P.,Schneider,N.S.; Macromolecules 8 (1) 68 (1975).

14. Seymour,R.W.,Estes,G.M.,Cooper,S.L.;Macromolecules 3 (5) 579 (1970).

15. Harrell,L.L.,Jr.;Macromolecules 2 (6) 607 (1969).

16. Srichatrapimuk,V.W.,Cooper,S.L.;J.Macromol.Sci.Phys. B15 (2) 267 (1978).

17a.Burchell,D.J.,Lasch,J.E.,Farris,R.J.,Hsu,S.L.;Polymer 23 965 (1982).

17b.Burchell,D.J.,Lasch,J.E.,Dobrovolny,E.,Page,N.,Domian,J.,Farris, R.J.,Hsu,S.L.;Appl.Spect. 38 (3) 343 (1984).

17c.Lasch,J.E.,Burchell,D.J.,Masoaka,T.,Hsu,S.L.;Appl.Spect. 38 (3) 351

(1984).

17d. Molis,S.E.,MacKnight,W.J.,Hsu,S.L.;Appl.Spect. <u>38</u> (4) 529 (1984).

17e. Burchell,D.J.,Hsu,S.L.;Adv. in Chem. <u>203</u> 533 (1983),C. Craver, Ed.

17f. Lasch,J.E.,Masoaka,T.,Burchell,D.J.,Hsu,S.L.;Polymer Bulletin <u>10</u> 51 (1983).

18. Siesler,H.W.;Polymer Bulletin <u>9</u> 382, 471, 557 (1983).

19. Skrovanek,D.J.,Howe,S.E.,Painter,P.C.,Coleman,M.M.;Macromolecules <u>18</u> (9) 1676 (1985).

20. Skrovanek,D.J.,Painter,P.C.,Coleman,M.M.;Macromolecules <u>19</u> (3) 699 (1986).

21. Coleman,M.M.,Lee,K.H.,Skrovanek,D.J.,Painter,P.C.;Macromolecules <u>19</u> (8) 2149 (1986).

22. Hesketh,T.R.,van Bogart,J.W.C.,Cooper,S.L.;Poly.Eng.Sci. <u>20</u> (3) 190 (1980).

23. van Bogart,J.W.C.,Bluemke,D.A.,Cooper,S.L.;Polymer <u>22</u> 1428 (1981).

24. Dominguez,R.J.G.;Poly.Eng.Sci. <u>21</u> (18) 1210 (1981).

25. Kwei,T.K.;J.Appl.Poly.Sci. <u>27</u> 2891 (1982).

26. Leung,L.M.,Koberstein,J.J.;Macromolecules <u>19</u> (3) 706 (1986).

27. Zdrahala,R.J.,Gerkin,R.M.,Hager,S.L.,Critchfield,F.E.;J.Appl.Poly. Sci. <u>24</u> 2041 (1979).

28. Chang,A.L.,Briber,R.M.,Thomas,E.L.,Zdrahala,R.J.,Critchfield,F.E.; Polymer <u>23</u> 1060 (1982).

29. Wilkes,C.E.,Yusek,C.S.;J.Macromol.Sci.Phys. <u>B7</u> (1) 157 (1973).

30. Schneider,N.S.,Desper,C.R.,Illinger,J.L.,King,A.O.,Barr,D.; J.Macromol.Sci.Phys. $\underline{B11}$ (4) 527 (1975).

31. Fulcher,K.U.,Corbett,G.E.;Brit.Poly.J. $\underline{7}$ 225 (1975).

32. Ophir,Z.,Wilkes,G.L.;J.Poly.Sci.Poly.Phys. $\underline{18}$ 1469 (1980).

33. Bonart,R.,Morbitzer,L.,Hentze,G.;J.Macromol.Sci.Phys. $\underline{B3}$ (2) 337 (1969).

34. Bonart,R.,Morbitzer,L.,Muller,E.H.;J.Macromol.Sci.Phys. $\underline{B9}$ (3) 447 (1974).

35. Koberstein,J.T.,Stein,R.S.;J.Poly.Sci.Poly.Phys. $\underline{21}$ 1439 (1983).

36. Leung,L.M.,Koberstein,J.T.;J.Poly.Sci.Poly.Phys. $\underline{23}$ 1883 (1985).

37. Koberstein,J.T.,Russell,T.P.;Macromolecules $\underline{19}$ (3) 714 (1986).

38. Blackwell,J.,Gardner,K.H.;Polymer $\underline{20}$ 13 (1979).

39. Blackwell,J.,Ross,M.;J.Poly.Sci.Poly.Lett. $\underline{17}$ 447 (1979).

40. Blackwell,J.,Nagarajan,M.R.;Polymer $\underline{22}$ 202 (1981).

41. Blackwell,J.,Nagarajan,M.R.,Hoitink,T.B.;Polymer $\underline{22}$ 1534 (1981).

42. Blackwell,J.,Lee,C.D.;J.Poly.Sci.Poly.Phys. $\underline{21}$ 2169 (1983).

43. Blackwell,J.,Lee,C.D.;Adv.Urethane Sci.Tech. $\underline{9}$ 25 (1984).

44 Blackwell,J.,Lee,C.D.;J.Poly.Sci.Poly.Phys. $\underline{22}$ (4) 759 (1984).

45. Blackwell,J.,Nagarajan,M.R.,Hoitink,T.B.;Polymer $\underline{23}$ 950 (1982).

46. Hocker,J.,Born,L.;J.Poly.Sci.Poly.Lett. $\underline{17}$ 723 (1979).

47. Born,L.,Hespe,H.,Crone,J.,Wolf,K.H.;Coll.Poly.Sci. $\underline{260}$ 819 (1982).

48. Born,L.,Crone,J.,Hespe,H.,Muller,E.H.,Wolf,K.H.;J.Poly.Sci. Poly.Phys. $\underline{22}$ 163 (1984).

49. Blackwell,J.,Quay,J.R.,Nagarajan,M.R.,Born,L.,Hespe,H.;J.Poly.Sci. Poly.Phys. $\underline{22}$ 1247 (1984).

50. Camberlin,Y.,Pascault,J.P.,Letoffe,J.M.,Claudy,P.;J.Poly.Sci.

Poly.Chem. 20 383 (1982).

51. Camberlin,Y.,Pascault,J.P.,Letoffe,J.M.,Claudy,P.;J.Poly.Sci.

    Poly.Chem. 20 1445 (1982).

52. Briber,R.M.,Thomas,E.L.;J.Macromol.Sci.Phys. B22 (4) 509 (1983).

53. Briber,R.M.,Thomas,E.L.;J.Poly.Sci.Poly.Phys. 23 1915 (1985).

54. Rustad,N.E.,Krawiec,R.G.;J.Appl.Poly.Sci. 18 401 (1974).

55. Minoura,Y.,Yamashita,S.,Okamoto,H.,Matsuo,T.,Izawa,M.,Kohmeto,S.;

    J.Appl.Poly.Sci. 22 1817,3101 (1978), 23 1137 (1979).

56. Klempner,D.,Frisch,K.C.;Adv.Urethane Sci.Tech. 8 93 (1981).

57. Schollenberger,C.S.,Stewart,F.D.;J.Elastoplastics 4 294 (1972).

58. Allen,N.S.,McKellar,J.F.;J.Appl.Poly.Sci. 20 1441 (1976).

59. Beachell,H.C.,Chang,I.L.;J.Poly.Sci.A-1 10 503 (1972).

60. Byrne,C.A.,Mack,D.P.,Sloan,J.M.;Rubber Chem.Tech. 58 985 (1985).

61. Byrne,C.A.;Adv.Elast.Rubber Tech.,Ed. J. Lal and J. E. Mark, Plenum

    Press, New York, N. Y., in press.

62. Singh,B.,Chang,L.W.,Forgione,P.S.;U.S.Patent 4,439,616 Mar. 27, 1984

    Tertiary Aralkyl Urethanes and Isocyanates Derived Therefrom

63. Robins,J.,Edwards,B.H.,Tokach,S.K.;Adv.Urethane Sci.Tech. 9 65

    (1984).

64. Christenson,C.P.,Harthcock,M.A.,Meadows,M.D.,Spell,H.L.,Howard,W.L.,

    Creswick,M.W.,Guerra,R.E.,Turner,R.B.;J.Poly.Sci.Poly.Phys. 24

    1401 (1986).

65. Silvestein,R.M.,Bassler,G.C.,Morrill,T.C.; Spectrometric Identifi-

    cation of Organic Compounds, Fourth Ed., John Wiley & Sons (1981).

66. Jasinski,J.P.,Desper,C.R.,Zentner,B.A.;   A Model Compound for Diol Linked TMXDI Units in Polyurethane Hard Segments: (I) The Structure of Diethyl-p-Tetramethylxylene Diurethane   submitted to Acta Crystallographica.

67. Alesi,A.L.,Houghton,W.W.,Roylance,M.E.,Simoneau,R.W.;   Evaluation of Polyurethane Elastomers for Applicatio in Vehicle Tracks,   AMTL internal report.

68. Yang,W.P.,Macosko,C.W.,Wellinghoff,S.T.; Polymer 27 1235 (1986).

69. Rubner,M.F.;Macromolecules 19 (8) 2114,2129 (1986).

AD-A178 312   SYNTHESIS AND PROPERTIES OF ALPHATIC POLYURETHANES AND   2/2
                MODEL COMPOUNDS CO..(U) ARMY LAB COMMAND WATERTOWN MA
                MATERIAL TECHNOLOGY LAB B A ZENTNER JAN 87 MTL-TR-87-3

UNCLASSIFIED   F/G 7/3   NL

‖‖ 1.0	2.8	2.5
	3.2	2.2
	3.6	
‖ 1.1	4.0	2.0
		1.8
‖ 1.25	‖ 1.4	‖ 1.6
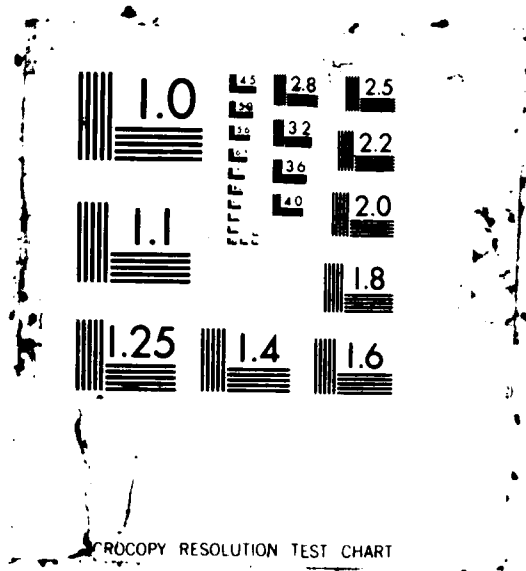
MICROCOPY RESOLUTION TEST CHART

XI. ACKNOWLEDGMENTS

DISTRIBUTION LIST

No. of Copies	To
1	Office of the Under Secretary of Defense for Research and Engineering, The Pentagon, Washington, DC 20301

Commander, U.S. Army Laboratory Command, 2800 Powder Mill Road, Adelphi, MD 20783-1145
1   ATTN: SLCIS-IM-TL

Commander, Defense Technical Information Center, Cameron Station, Building 5, 5010 Duke Street, Alexandria, VA 22304-6145
2   ATTN: DTIC-FDAC

1   Metals and Ceramics Information Center, Battelle Columbus Laboratories, 505 King Avenue, Columbus, OH 43201

U.S. Army Aviation Systems Command, 4300 Goodfellow Boulevard, St. Louis, MO 63120-1798
1   ATTN: AMCPM-BH, COL Ralph H. Lauder, Program Manager, BLACKHAWK
1   AMCPM-CO, Mr. William H. Barthel, Acting Program Manager, COBRA
1   Mr. William McClane

Department of the Army, U.S. Army Research, Development and Standardization Group (UK), Box 65 FPO, New York, NY 09510
1   ATTN: Dr. Iqbal Ahmad

Commander, Army Research Office, P.O. Box 12211, Research Triangle Park, NC 27709-2211
1   ATTN: Information Processing Office
1   Dr. Eugene E. Magat, Chief, Polymer Chemistry Division

Commander, U.S. Army Chemical Research and Development Center, Aberdeen Proving Ground, MD 21010
1   ATTN: SMCCR-RSP-P, A. Stuempfle
1   SMCCR-RSC-C, W. Shuely
1   SMCCR-PPI, D. English
1   SMCCR-PPD, J. Baker
1   SMCCR-MSS, J. Seigh

Commander, U.S. Army Materiel Command (AMC), 5001 Eisenhower Avenue, Alexandria, VA 22333
1   ATTN: AMCLD
1   AMCLD-SC, H. Comminge

Commander, U.S. Army Materiel Systems Analysis Activity, Aberdeen Proving Ground, MD 21005
1   ATTN: AMXSY-MP, H. Co. :n

Rock Island Arsenal, Rock Island, IL 61299-5000
1   ATTN: SMCRI-EN, Mr. Walter Kisner

No. of Copies	To

Commander, U.S. Army Mobility Equipment Research and Development Command, Fort Belvoir, VA 22060
1 ATTN: STRBE-VU, P. Touchet
1   STRBE-VU, P. Gatza
1   STRBE-VU, G. Rodriquez

David Taylor Naval Ship Research and Development Center, Annapolis, MD 21402
1 ATTN: Code 2801, Mr. Joseph R. Crisci, Assistant Department Head for Research
1   Code 2842, Mr. Marshall M. Sherman
1   Code 2842, Mr. William M. Widenor

Naval Research Laboratory, Washington, DC 20375
1 ATTN: Code 6120, Dr. Robert Fox

Chief of Naval Research, Arlington, VA 22217
1 ATTN: Code 431, L. Peebles
1   Code 413, K. Wynne

Naval Weapons Center, China Lake, CA 93555
1 ATTN: Mr. Robert Rhein

1 Edward J. Morrissey, AFWAL/MLTE, Wright-Patterson Air Force Base, OH 45433

Commander, U.S. Air FOrce Wright Aeronautical Laboratories, Wright-Patterson Air Force Base, OH 45433
1 ATTN: AFWAL/MLC
1   AFWAL/MLLP, M. Forney, Jr.
1   AFWAL/MLBC, Mr. Stanley Schulman
1   AFWAL/MLBT, Mr. J. Sieron

National Aeronautics and Space Administration, Langley Research Center, Hampton, VA 23665
1 ATTN: Mr. T. L. St. Clair, Materials Division

National Aeronautics and Space Administration, Marshall Space Flight Center, Huntsville, AL 35812
1 ATTN: R. J. Schwinghammer, EH01, Dir, M&P Lab
1   Mr. W. A. Wilson, EH41, Bldg. 4612

Department of Defense, Materials Research Laboratories, Elastomers and Plastics Group, P.O. Box 50, Ascot Vale, Victoria 3032, Australia
1 ATTN: Mr. T. E. Symes

National Bureau of Standards, Gaithersburg, MD 20899
1 ATTN: Dr. Gregory McKenna, Polymer Division

Lawrence Livermore National Laboratories, P.O. Box 808, Livermore, CA 94550
1 ATTN: Mr. Alfred Goldberg, Engineering Sciences Division

Commander, U.S. Army Electronics Research and Development Command, Fort Monmouth, NJ 07703
1 ATTN: AMDSD-L
1   AMDSD-E

No. of Copies	To

Commander, U.S. Army Missle Command, Redstone Arsenal, AL 35898
1 ATTN: AMSMI-RKP, J. Wright, Bldg. 7574
1 AMSMI-TB, Redstone Scientific Information Center
1 AMSMI-RLM
1 Technical Library

Commander, U.S. Army Armament, Munitions and Chemical Command, Dover, NJ 07801
2 ATTN: Technical Library
1 AMDAR-SCM-O, A. Tatyrek
1 AMDAR-LCA, Mr. Harry E. Pebly, Jr., PLASTEC, Director

Commander, U.S. Army Natick Research, Development and Engineering Center, Natick, MA 01760
1 ATTN: Technical Library
1 STRNC-ITP, J. Brennick
1 STRNC-ITP, R. Laible
1 STRNC-ITP, G. Wilusz

Commander, U.S. Army Tank-Automotive Command, Warren, MI 48090
2 ATTN: AMSTA-TSL, Technical Library
1 AMSTA-RCKT, A. Pacis
1 AMSTA-RCKT, J. Patt
1 AMSTA-RCKT, G. Szakacs
1 AMSTA-RCK, M. Kaifish
1 AMSTA-NR, R. Case
1 AMSTA-GBP, M. Hoffman
1 AMSTA-ZSA, D. Rose

Commander, White Sands Missle Range, NM 88002
1 ATTN: STEWS-WS-VT

Commander, Combat Systems Test Activity, Aberdeen Proving Ground, MD 21005-5059
1 ATTN: STEAP-MT-D, K. Jones

Commander, Dugway Proving Ground, Dugway, UT 84022
1 ATTN: Technical Library, Technical Information Division

Commander, Harry Diamond Laboratories, 2800 Powder Mill Road, Adelphi, MD 20783
1 ATTN: Technical Information Office

California Institute of Technology, 4800 Oak Grove Drive, Pasadena, CA 91109
1 ATTN: Dr. Robert F. Landel, Jet Propulsion Laboratory, Applied Mechanics Technology Section

Detroit Diesel Allison, Dept. 841, K-15, 13400 W. Outer Drive, Detroit, MI 48239-4001
1 ATTN: D. E. Larkin

Director, U.S. Army Materials Technology Laboratory, Watertown, MA 02172-0001
2 ATTN: SLCMT-IML
1 Author

AD _____

U.S. Army Materials Technology Laboratory,
Watertown, Massachusetts 02172-0001
SYNTHESIS AND PROPERTIES OF ALIPHATIC
POLYURETHANES AND MODEL COMPOUNDS
CONTAINING $\alpha,\alpha,\alpha',\alpha'$-TETRAMETHYL-p-
XYLYLENE-DIISOCYANATE
Brian A. Zentner

Key Words

Polyurethanes
X-ray crystallography
Fatigue (mechanics)

Tetramethylxylene-diisocyanate is a new compound undergoing experimental testing as a component in the manufacture of polyurethanes. It is examined as a possible replacement for the styrene-butadiene formulas currently used in tank treads. Several samples have been prepared which contain varying ratios of ingredients and percentages of hard segment material. Compressive fatigue tests have shown the block samples to be resistant to hysteretic heatup provided they contain a certain minimum percentage of hard segment material. Model compounds have been analyzed by X-ray crystallography to determine the probable orientation of the chains in these hard segment regions.

END

4-87

DTIC